INVESTIGATIONS INTO APPLYING THE TRANSMISSION SIMULATOR METHOD OF HYBRID MODAL SUBSTRUCTURING TO MODEL AN ELECTRODYNAMIC SHAKER

by

Benjamin John Moldenhauer

A thesis submitted in partial fulfillment of the requirements for the degree of

Master of Science

(Engineering Mechanics)

at the

UNIVERSITY OF WISCONSIN - MADISON

2018

Abstract

When conducting a vibration test with an electrodynamic shaker, the layout of fixtures and test components on the shaker adapter inherently alters the vibration modes and anti-resonances of the system. During a test, these dynamics can be excited by the shaker itself, leading to an invalid test if the desired environment is exceeded at some points, and potentially damaging the shaker or test components. A high-fidelity shaker model would allow for accurate pretest planning in which test component layout and control accelerometer placement can be optimized to mitigate problem areas. However, shaker systems are notoriously difficult to model analytically due to a multitude of joints with indefinite properties, unknown stiffness and damping of the magnetic field, and the scarcity of available technical drawings for the internal components.

This thesis explores the use of hybrid modal substructuring to create a test-based model of a shaker table with an attached shaker fixture. The transmission simulator method is used to decouple a finite element model of the fixture from an experimentally derived modal model of the shaker and fixture and replace it with a finite element model of the fixture with an attached test article. This produces a predictive model of the dynamics of the total system, consisting of the shaker, fixture, and test article. Three test cases are explored, in which fixtures and test articles of increasing complexity are implemented to probe the limits of the proposed model creation strategy.

In the first case, a circular aluminum plate and rectangular steel block are used as the fixture and test article, respectively. While quite simple, this setup demonstrated the usability and accuracy of the proposed process and allowed a general framework for it to be developed.

The second case implemented a three-sided half cube fixture with a cantilever beam as the test article. Special care was taken to ensure that an optimized test layout and accurate FEMs were created. This setup verified the effectiveness of the substructuring process in preserving the dynamics of a more complex fixture while successfully including the test component dynamics through the usable frequency range of the shaker.

The third case sought to impose a significant change to the fixture dynamics to validate the accuracy of the process through significant system deviations. This was done by attaching the steel block from case 1 to the half cube instead of the beam. Results indicate that the additional localized mass is accounted for and the response of the system on the block can be reasonably predicted from the hybrid model.

These test cases provide compelling evidence as to the accuracy and practicality of modeling an electrodynamic shaker through its usable frequency range with the transmission simulator method. Future work can be done to further refine the substructuring process, in selecting suitable basis modes for each subsystem, improving damping estimations, and establishing general metrics to quantify the accuracy of the model when no truth data is known a priori.

Acknowledgements

This work was funded by the Plant Direct Research and Development (PDRD) program of Honeywell Federal Manufacturing & Technologies, LLC, which manages and operates the Department of Energy's Kansas City National Security Campus under contract DE-NA0000622. My personal thanks go to Washington DeLima and Eric Dodgen, who supported this project from its onset and offered many useful real-world insights for its application that would have otherwise gone unnoticed.

Special thanks are owed to my adviser, Dr. Matthew Allen, for allowing me the opportunity to perform this research and learn under his guidance. I would not be in this position without his infinite patience, generosity, and kindness, and am much better off because of it. There is also the small fact that he and Randy Mayes from Sandia National Labs established the theoretical basis this entire body of work is based on. None of this would have been possible without Dr. Allen.

Last but absolutely not least, I would like to thank cats, and also all my friends and family for supporting me in all of my endeavors, and my colleagues for their assistance with solving numerous MATLAB errors, Abaqus intricacies, and homework assignments.

Contents

1. Introduction

1.1. Motivation

Structures that experience extreme vibrational loads during their service life are typically validated by performing life tests on a shaker. A shaker is able to generate arbitrary frequency and amplitude content that can be defined to recreate whatever environment the structure is likely to encounter. However, the shaker will also experience these environments as it produces them, possibly exciting its own resonances. Furthermore, to provide the necessary excitation, the shaker must be directly attached to the structure, creating a coupled system. The nature of this coupling can alter the dynamics of the shaker in such a way that it may respond to its own excitation in an unexpected manner. This can lead to invalid test results or possibly damage to the test article and/or the shaker.

A model of the coupled test system that captures the cumulative response of the complete assembly would provide insight into how the test article alters the response of the shaker and form a basis for predictive design of the test setup and allow for a more robust test plan. Unfortunately, high fidelity numerical models of shakers, i.e. a finite element model (FEM), are notoriously difficult to create, due to the multitude of unknowns present in the structure, such as joint properties, material parameters, and internal layout [1, 2, 3]. Purely experimentally derived models are also unlikely to be effective as they are time consuming to create, are situationally

specific, and require a test setup and plan to have already been created and implemented, negating the need for a predictive model.

The research presented here within pertains to generating a hybrid experimental-analytical model of a shaker that effectively circumvents the difficulties mentioned above by leveraging the strengths of each method. This is done using the transmission simulator method (TSM) of modal substructuring, also known as modal constraints for fixture and subsystem (MCFS) [4, 5]. With this technique, an experimental model of the shaker with a test fixture can be used as a basis to which FEMs of the test fixture and any test articles can be coupled, yielding a model of the full system. This experimentally captures the dynamics of the internal shaker components and the linear stiffness and damping characteristics of the joints between the test fixture and the shaker, removing the need to accurately model them analytically. Also, by using FEMs of the fixture and potential test article, many different test configurations can be quickly simulated, avoiding costly prototyping and testing.

1.2. Research Contributions

The goal of this research was to implement an existing theoretical framework for experimental substructuring, the transmission simulator method, to generate a predictive model of an electrodynamic shaker. In the most basic sense, this meant collecting the necessary experimental and finite element model data and performing the established calculations to produce a model of a potential shaker setup. Over the

course of completing this process on several different test cases, some general conclusions can be drawn. First, the TSM operated correctly in every test case; the response of the shaker assembly could be adequately predicted through its operable frequency span. A commonly accepted rule of thumb for this type of substructuring is that dynamic information out to twice the target frequency range is needed; in the current work, this generally proved true as well. Furthermore, in selecting a specific set of basis modes to represent each subsystem, some observations can be stated. For the transmission simulator finite element model, modes that correlate well with experimental data, in mode frequency, shape and scaling, formed an effective basis set. However, if an included mode had a higher number than the number of points used to define it, the TSM model would become wildly inaccurate, possibly due to aliasing of the shape. For the analytical subsystem, it was found that adding enough modes to slightly surpass the highest mode frequency included in the transmission simulator basis set provided the best results. Adding additional modes did not severely degrade results but did generally lower predicted frequencies past truth values. By defining each subsystem with the maximum number of accurate modes possible, the TSM is able to augment the supplied experimental subsystem data and produce a viable model of various proposed test setups.

1.3. Thesis Structure

This thesis is divided into several sections, starting with an overview of dynamic substructuring and a summary of the theory behind the TSM. The following

three sections describe the three test cases that were implemented to investigate the applicability of the TSM to modeling an electrodynamic shaker. Each is divided into subsections detailing the various steps required to generate the shaker model. First, physical descriptions of each subsystem are given, including the dimensions, materials, and mass. Next, the test procedure that was developed to acquire and process experimental data is defined. This includes sensor and excitation locations, equipment utilized, and a discussion of the recorded data. Also, the process employed to create the necessary finite element models is given, including mesh generation, updating of material properties and contact areas, and model validation with respect to experimental data. Finally, with all the necessary information to perform the TSM substructuring, the resultant experimental/analytical shaker model is evaluated relative to experimental truth data. Following the test cases, conclusions pertaining to the accuracy and capability of implementing the TSM to efficiently model electrodynamic shakers are given, along with possible paths for future work.

Section 3, which describes test case 1, is an updated version of the process and results given in [6], a conference paper written by the author for the 36th International Modal Analysis Conference (IMAC). Section 2, which provides a brief theoretical background on substructuring, and section 4, which details test case 2, have largely been compiled from [7], an additional conference paper written by the author for the 37th IMAC.

2. Theory

2.1. Dynamic Substructuring

Modeling and analyzing system dynamics becomes increasingly difficult as the size and complexity of the structure grows. Large FEMs can require an unreasonable amount of time and computational power to directly solve, and as the assembly becomes larger and more complicated it becomes more difficult to design and perform an experiment that can capture all the modes of interest. However, these difficulties can be somewhat alleviated by dividing the structure into smaller, more manageable subcomponents that may be analyzed individually in whatever domain is most appropriate, e.g. experimental or analytical. When one of the components is experimental, the methods used to combine experimental and numerical models to predict the response of the coupled system are termed experimental dynamic substructuring [8, 9].

Experimental dynamic substructuring methods are divided into two groups: Frequency-Based Substructuring (FBS) and Component Mode Synthesis (CMS). FBS uses the frequency response functions (FRFs) of the subcomponents to predict the response of the assembled system. CMS, also known as Modal Substructuring, combines the subcomponent equations of motion in modal coordinates to build the equation of motion of the assembled system. In the research presented herein, this is achieved using the Transmission Simulator Method [10].

While the CMS methods differ in which component's modes are chosen to represent the subcomponent, it is imperative that the component modes of the individual subcomponents form an adequate basis to represent the motion of the coupled assembly.

2.2. Transmission Simulator Method

The Transmission Simulator Method (TSM), as proposed by Allen, Mayes, et al. [4, 5, 11], allows for experimental and analytical models to be coupled together through a common subcomponent that is present in both. This component, referred to as the Transmission Simulator (TS), acts as a distributed interface between the experimental and analytical subsystems, allowing their coupling constraints to be satisfied by the modal dynamics of the TS, as opposed to the more difficult process of enforcing compatibility in all six physical degrees of freedom at each point on the surface of the interface. Also, the TS effectively mass-loads the interface between the other subsystems and simulates the forces that would act there in the assembled structure. In practice, an experimental model is obtained by performing a modal test on some physical system that includes the TS. By decoupling a FEM of the TS from this model, the physical presence of the TS is removed, while the dynamics of a loaded interface remain in the physical component model. If this same process is carried out on a FEM that includes the TS and a third subcomponent, an analytical model of that subcomponent with a mass loaded interface is produced. The experimental and analytical models with mass loaded interfaces can then be

coupled together with CMS, yielding a hybrid experimental/analytical model of the assembled structure.

This research applies the TSM to create a model of a floor-mounted electromagnetic shaker that has a shaker fixture mounted to the armature and a mock test article attached to the fixture. The shaker with the fixture is the experimental subsystem, the fixture is the TS, and the prospective test article together with the fixture is the analytical subsystem. Figure 1 displays a schematic of the effective process that will be completed. Essentially, from an initial experimental modal model of the shaker and fixture, the fixture will be removed and replaced by a FEM of the fixture with the test article, yielding a hybrid model predicting the response of the complete assembly. The test cases presented in Sections 3, 4, and 5 detail the TSM performed on several combinations of fixtures and test articles with increasing levels of complexity in both subcomponents.

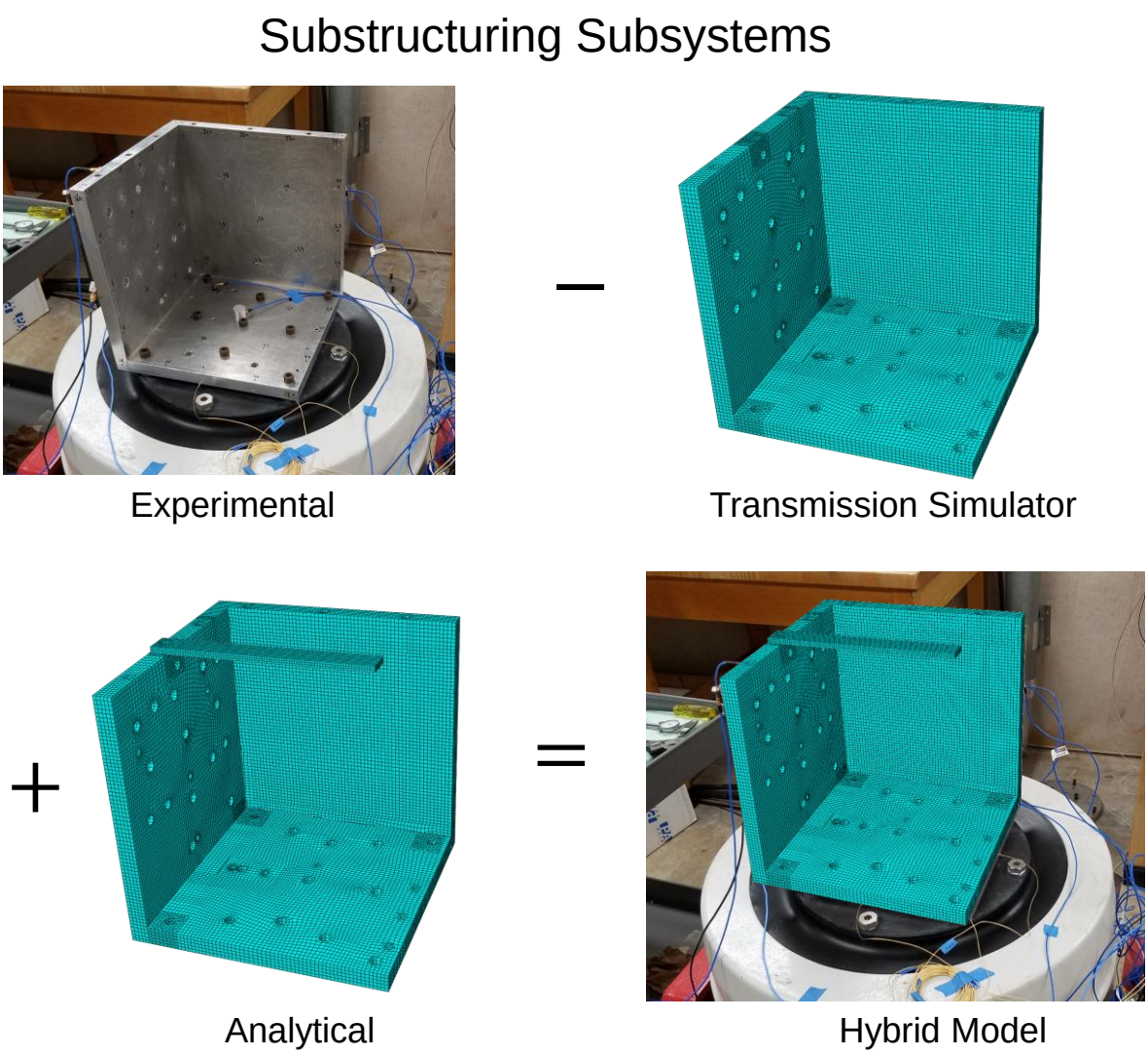

Figure 1: Transmission Simulator Method Schematic and Subsystems

2.3. Mathematical Basis

To combine the subsystems, the equations of motion for each are first formulated in terms of modal coordinates, as given in Eq.(1) [10], where damping is neglected for brevity. In this equation, $\boldsymbol{\omega}$ is frequency, $\mathbf{I}$ is an appropriately dimensioned identity matrix, $\boldsymbol{\eta}$ are generalized modal coordinates vectors, $[\boldsymbol{\omega}_{\mathbf{n}}]$ are

diagonal matrices of subsystem natural frequencies, $\boldsymbol{\phi}^{\mathbf{T}}$ are transposed subsystem mode shape matrices, and $\mathbf{F}$ are vectors of applied forces. The terms representing the TS are negative to signify that this subsystem is being removed, while the experimental and analytical FEM subsystems are being coupled.

$$-\boldsymbol{\omega}^{\mathbf{2}}\begin{bmatrix}\mathbf{I_{EX}} & \mathbf{0} & \mathbf{0}\\ \mathbf{0} & -\mathbf{I_{TS}} & \mathbf{0}\\ \mathbf{0} & \mathbf{0} & \mathbf{I_{AN}}\end{bmatrix}\begin{bmatrix}\boldsymbol{\eta}_{\mathbf{EX}}\\ \boldsymbol{\eta}_{\mathbf{TS}}\\ \boldsymbol{\eta}_{\mathbf{AN}}\end{bmatrix}+\begin{bmatrix}\left[\boldsymbol{\omega}^{\mathbf{2}}_{\mathbf{n,EX}}\right] & \mathbf{0} & \mathbf{0}\\ \mathbf{0} & \left[-\boldsymbol{\omega}^{\mathbf{2}}_{\mathbf{n,TS}}\right] & \mathbf{0}\\ \mathbf{0} & \mathbf{0} & \left[\boldsymbol{\omega}^{\mathbf{2}}_{\mathbf{n,AN}}\right]\end{bmatrix}\begin{bmatrix}\boldsymbol{\eta}_{\mathbf{EX}}\\ \boldsymbol{\eta}_{\mathbf{TS}}\\ \boldsymbol{\eta}_{\mathbf{AN}}\end{bmatrix}=$$

$$\begin{bmatrix}\boldsymbol{\Phi}^{\mathbf{T}}_{\mathbf{EX}} & \mathbf{0} & \mathbf{0}\\ \mathbf{0} & -\boldsymbol{\Phi}^{\mathbf{T}}_{\mathbf{TS}} & \mathbf{0}\\ \mathbf{0} & \mathbf{0} & \boldsymbol{\Phi}^{\mathbf{T}}_{\mathbf{AN}}\end{bmatrix}\begin{bmatrix}\mathbf{F_{EX}}\\ \mathbf{F_{TS}}\\ \mathbf{F_{AN}}\end{bmatrix} \tag{1}$$

To enforce the coupling between the subsystems, a set of constraint equations is needed. Unlike more traditional substructuring methods, the TSM does not impose a strong physical constraint between the components in the physical degrees of freedom at the surface of their interface. Instead, constraints are enforced using the modal degrees of freedom of the TS, distributing the effective interface and softening the constraints [4, 5]. These constraint equations are given in modal form in Eq.(2), in which $\boldsymbol{\Phi}^{\dagger}$ denotes the Moore–Penrose pseudo-inverse of the mode shape matrix.

$$\begin{bmatrix}\boldsymbol{\Phi}^{\dagger}_{\mathbf{TS}} & \mathbf{0}\\ \mathbf{0} & \boldsymbol{\Phi}^{\dagger}_{\mathbf{TS}}\end{bmatrix}\begin{bmatrix}\boldsymbol{\Phi}_{\mathbf{EX}} & -\boldsymbol{\Phi}_{\boldsymbol{TS}} & \mathbf{0}\\ \mathbf{0} & -\boldsymbol{\Phi}_{\boldsymbol{TS}} & \boldsymbol{\Phi}_{\mathbf{AN}}\end{bmatrix}\begin{bmatrix}\boldsymbol{\eta}_{\mathbf{EX}}\\ \boldsymbol{\eta}_{\mathbf{TS}}\\ \boldsymbol{\eta}_{\mathbf{AN}}\end{bmatrix}=\mathbf{0} \tag{2}$$

From the subsystem natural frequencies and modeshape matrices and the constraint conditions, effective modal mass, damping, and stiffness matrices for the assembled structure can be found. The modal parameters of the assembly are found after performing an Eigen solution with the modal mass and stiffness matrices. For a more rigorous and complete derivation, see [4, 10].

3. Test Case 1: Circular Plate with Block

3.1. Subsystem Definitions

3.1.1. The Transmission Simulator

For the first test case, the TS subsystem is a simple aluminum plate, as shown in Figure 2. The plate is 13 inches in diameter, 1 inch thick, weighs 13.2 lbs, and attaches to the shaker with seventeen 3/8-inch steel bolts torqued to 22 ft-lbs. The plate was machined at UW – Madison to provide a more suitable configuration and size for the test article attachment points.

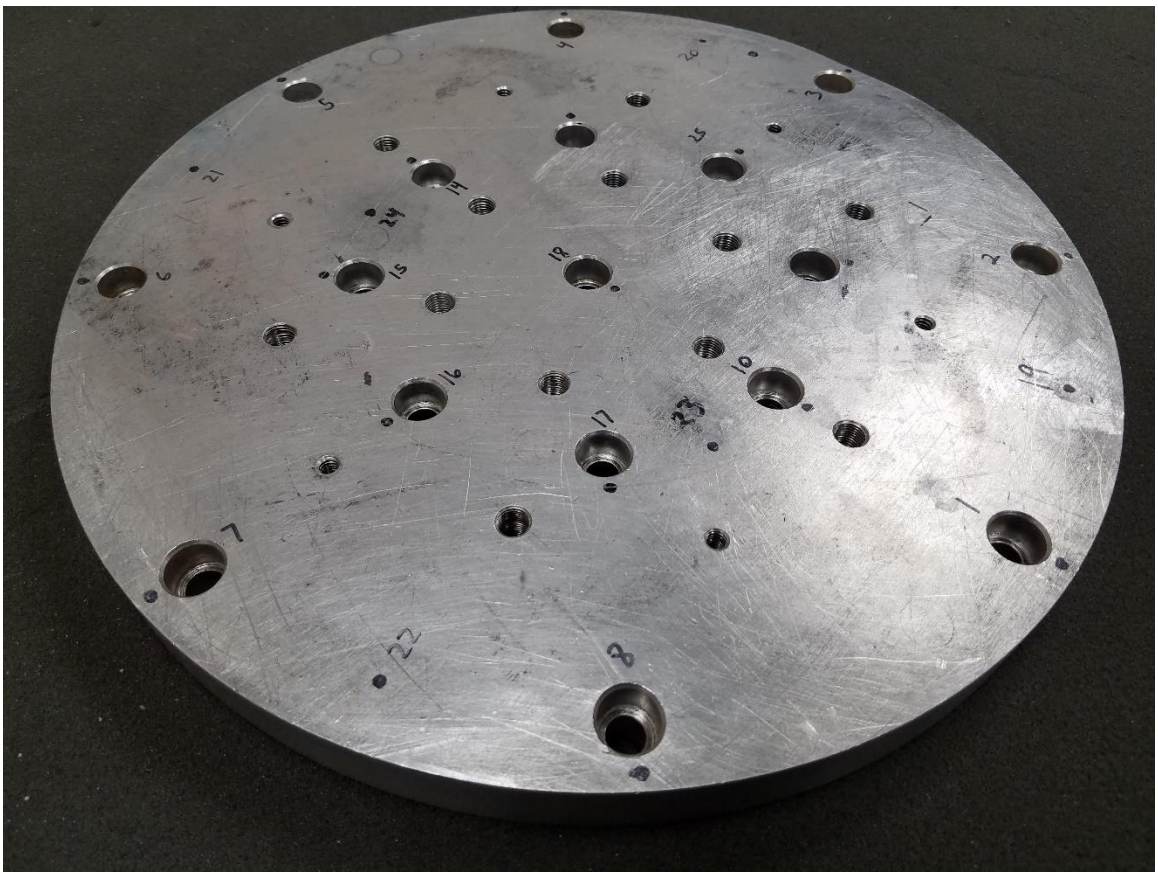

Figure 2: The Transmission Simulator, an aluminum adapter plate

3.1.2. Experimental Subsystem

In this work, the experimental subsystem is the TS mounted to an LDS V830 electromagnetic shaker, which is located at the University of Wisconsin – Madison. The shaker, as shown in Figure 3, consists of a top armature measuring 13 inches in diameter, features 21 total attachment points and, according to the manufacturer specifications, has a usable frequency span of 0-3000 Hz and can produce a maximum sine force of 2,200 lbs.

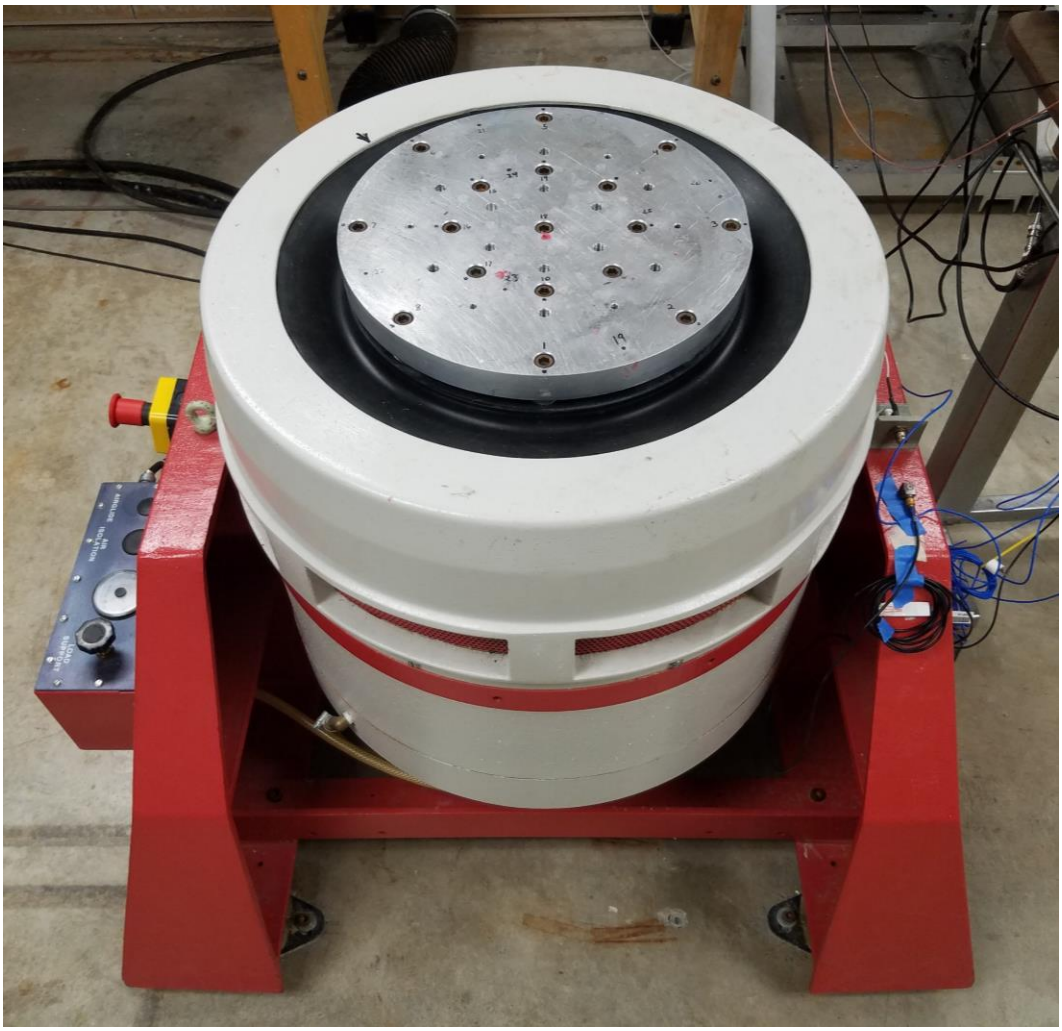

Figure 3: The Experimental Subsystem, the shaker and plate fixture

3.1.3. Analytical Subsystem

For the purposes of this initial proof-of-concept test case, a simple steel block was chosen for the mock test article in the analytical subsystem. The block is composed of generic stock steel, measures 2”x2”x4”, weighs 4.6 lbs, and was positioned on the aluminum adapter plate as shown in Figure 4, which depicts a CAD model of the block and TS. A physical copy of the block was also machined in order to acquire experimental truth data.

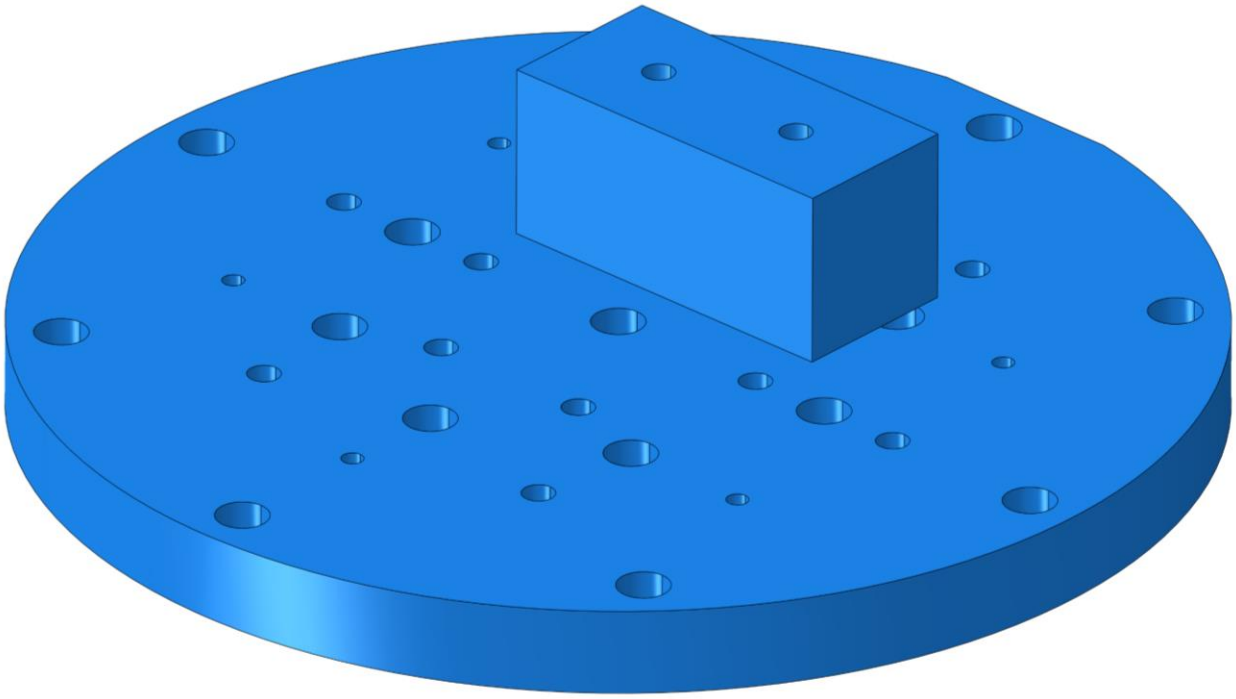

Figure 4: The Analytical Subsystem; a representative CAD model

3.2. Experimental Setup

Experimental modal data was gathered in the form of a roving hammer test. This was done to ensure that the frequency band of interest would be sufficiently excited and to provide a large array of potential drive points for mass normalizing the

experimental modeshapes. The locations of each accelerometer and hammer hit were positioned according to engineering judgement and are shown below in Figure 5. The hammer strikes marked by red circles were done in the vertical direction into the page and those given by the red arrows were applied radially inward on the outer edge of the plate toward the center. The accelerometers, marked by white dots, were placed midway between two hammer locations in order to assume a drive point value that is the average of the values on either side.

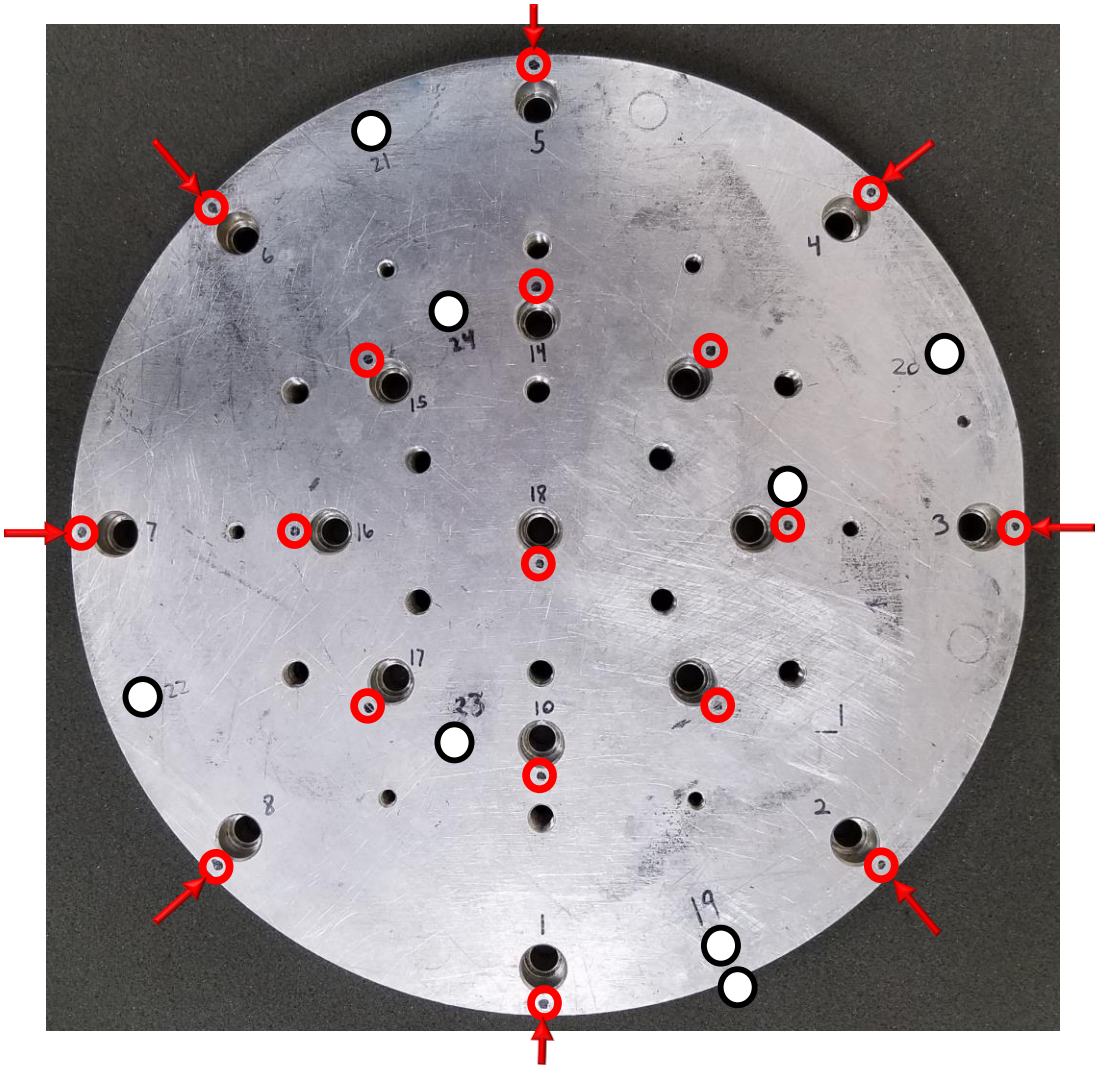

Figure 5: Roving Hammer and Accelerometer Locations

The accelerometer data was recorded in Data Physics SignalCalc® 830 software using the Data Physics Abacus® hardware interface. A frequency span of 0-5000 Hz was set to fully capture the operable range of the shaker. For impact excitation, a 086C04 PCB Modal Hammer was utilized. The test setup with all the aforementioned hardware is shown below in Figure 6.

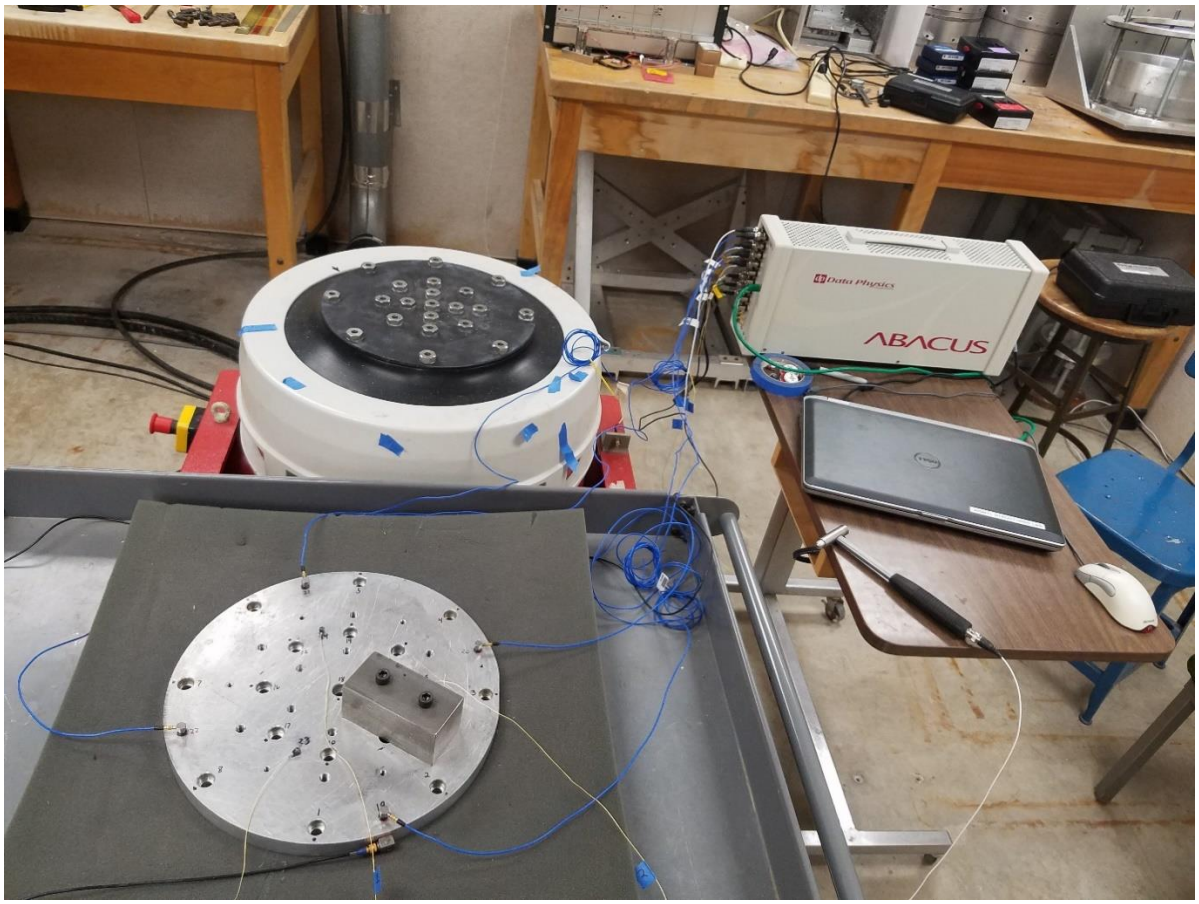

Figure 6: Test setup used to acquire experimental data for all test configurations

A modal test was performed on four configurations: the plate isolated on foam, the plate and the block bolted together and resting on foam, the plate attached to the shaker, and the plate with block attached to the shaker. The tests on foam simulate free conditions and provide data to validate their respective FEMs. Data

from the shaker and plate test is used as the experimental subsystem data for the TSM. The shaker, plate, and block test results are taken as truth data from which the substructuring results may be verified.

An overlay of the results from the foam test cases are shown in Figure 7. The FRFs shown are a composite of all hammer locations over all accelerometers. The modes near 2000 Hz and 4000 Hz, commonly called drum modes, are noticeably shifted in frequency. These display a heightened sensitivity to the presence of the block due to their greater excitation in the vertical translation direction, which now carries more inertial mass. The other modes, commonly called potato chip modes, are relatively unaffected in frequency by the presence of the block because these modes are more akin to rotations of the block. However, these rotations are the cause of the additional modes observed with the plate and block at 3000 Hz.

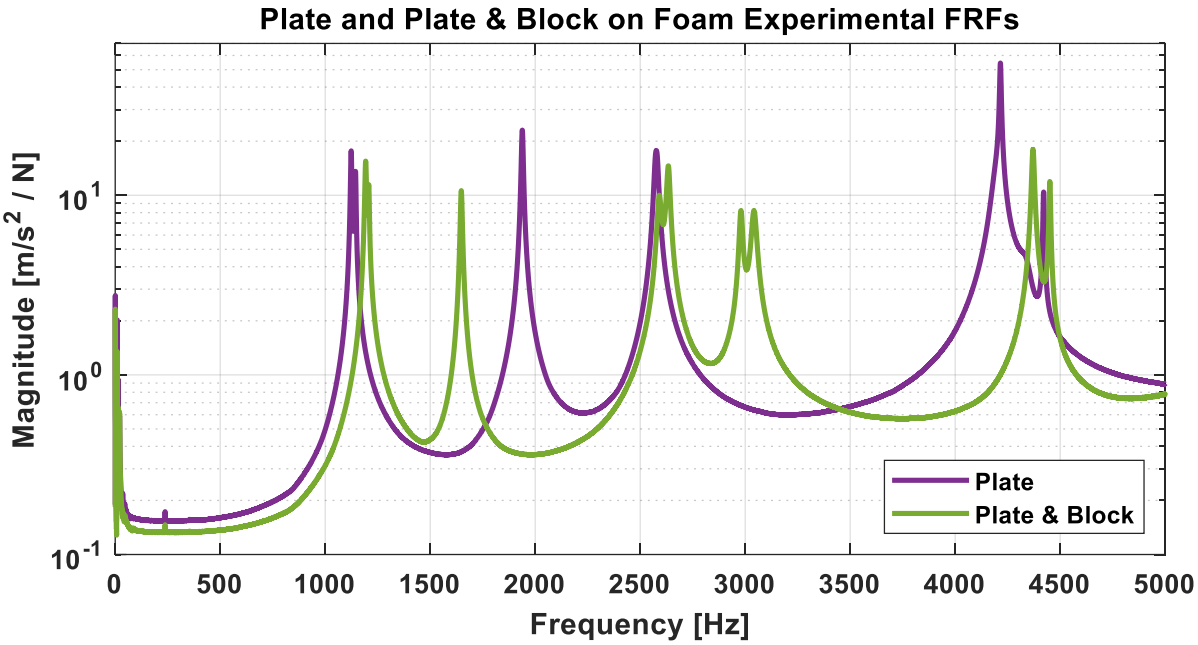

Figure 7: Modal test results for the plate and plate & block on foam

The on-shaker testing yields results that are drastically different than those previously discussed, as observed in Figure 8. Under approximately 2000 Hz, the response with and without the block is nearly identical, with a slight shift to lower frequencies and lower amplitude due to the additional weight of the block. Above 2000 Hz, the modes display a more significant lowering in frequency, with the peak at 2100 Hz completely splitting apart. Additionally, between 3000 Hz and 4000 Hz, many small peaks are created after adding the block. However, the shape of the all the modes are unlike the free plate modes and do not radically change with the presence of the block, implying that the plate and block have a very limited effect on the shaker beyond adding additional mass. The shaker armature is evidently much stiffer than the plate, making it the dominant component in the assembly; the plate simply deforms to whatever shape the armature is in.

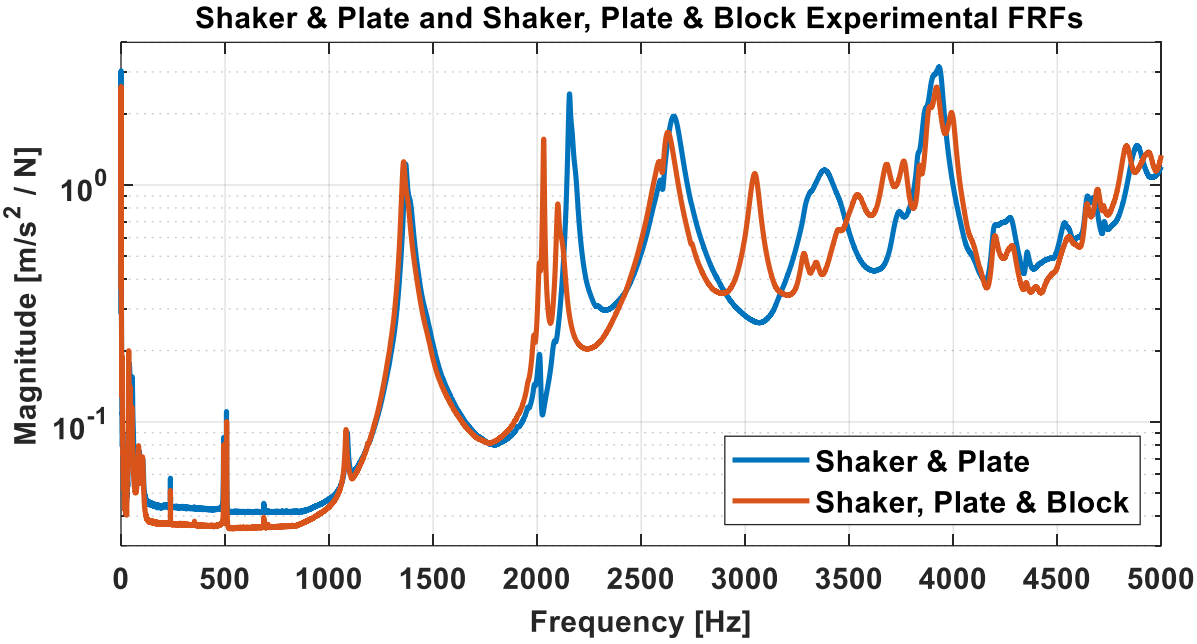

Figure 8: Modal test results for the Shaker test cases

Curve fitting for the experimental data was done using the Algorithm of Mode Isolation (AMI) [12, 13]. This program successively fits and subtracts modes from the experimental data until all significant peaks are accounted for. As an output, AMI supplies the natural frequencies, damping ratios, and state space modal residues for each mode. For the TSM, the mode shapes must be mass normalized. To extract these from the residues, first they are used to approximate the classical mode (i.e. real mode) residues and then the square root of the value at the drive point is used to scale the remaining values. This process is understood by observing the typical modal transfer function equation given below in Eq.(3), in which $\boldsymbol{\omega}$ is frequency, $\boldsymbol{\omega_n}$ is the natural frequency at mode $\mathbf{n}$, $\boldsymbol{\xi_n}$ is the damping ratio for mode $\mathbf{n}$, $\boldsymbol{\phi_n}$ is the mass normalized mode shape, and $\boldsymbol{\phi_{n,dp}}$ is the value of the mode shape at the drive point. The product $\boldsymbol{\phi_n \phi_{n,dp}}$ is the classical mode residue and is a matrix with rows corresponding to each hammer location and columns for each mode. The value for the drive point location is then equivalent to the square of the drive point value of the mass normalized mode shape, as in Eq.(4). This can be used to mass normalize the residue matrix as shown in Eq.(5).

$$\mathbf{H(\omega)} = \sum_{\mathbf{n=1}}^{\mathbf{\#\ modes}} \frac{\boldsymbol{\phi_n \phi_{n,dp}}}{\mathbf{-\omega^2 + i2\omega\xi_n\omega_n + \omega_n^2}} \tag{3}$$

$$\sqrt{\mathbf{residue_{n,dp}}} = \boldsymbol{\phi_{n,dp}} \tag{4}$$

$$\boldsymbol{\phi_n} = \frac{\mathbf{residue_n}}{\sqrt{\mathbf{residue_{n,dp}}}} \tag{5}$$

It is of note that each mode shape can be normalized relative to a different drive point. This can be advantages when certain drive points poorly excite a mode, in that a more suitable location can be chosen. For this work, the drive point with the largest value, $\boldsymbol{\phi_{n,dp}}$, was taken to normalize each respective mode.

3.3. Finite Element Analysis

For the substructuring procedure, FEMs of the adapter plate and the adapter plate and block were created. In the current work, this was done in Abaqus using solid 20-node hex elements, resulting in the mesh shown in Figure 9, containing 46,800 elements and 216,600 nodes.

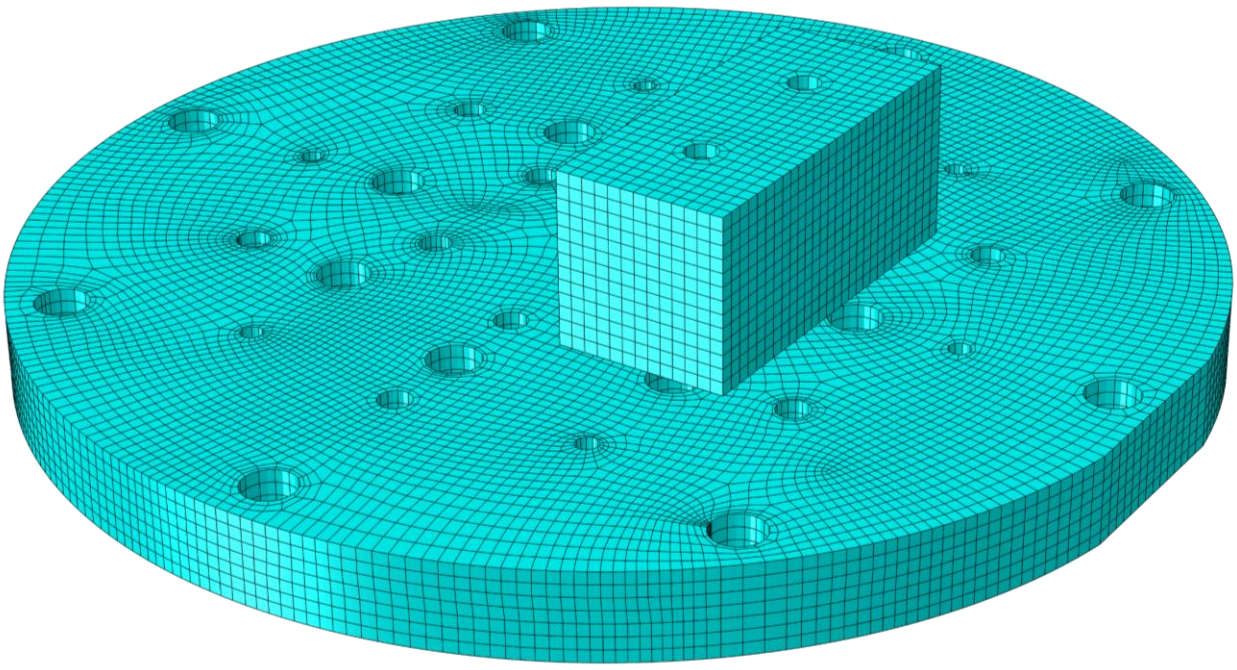

Figure 9: Analytical Subsystem FEM, Plate and Block

A modal solution was then performed in order to determine the natural frequencies of the models. By comparing these results to the experimental data

taken on foam for each subsystem, the material properties and the contact between the plate and the block were varied till good agreement was established between test and FEM. For the aluminum plate, an elastic modulus of 1e7 psi, density of .1 lbm/in^3, and Poisson's ratio of .33 were used. For the steel block, an elastic modulus of 2.9e7 psi, density of .28 lbm/in^3, and Poisson's ratio of .33 were used. The contact area between the plate and block was set to fully bonded in a square area approximately .5" around each hole, with frictionless no separation defined around this area to the edge of the block.

For the TS FEM, or the isolated plate in free conditions, Figure 10 shows a comparison between test and FEM. The top of the figure displays the experimental composite FRF from Figure 7 with black lines representing the FEM frequencies. For perfect agreement, the vertical lines would pass directly through the peaks in the FRF. For this model, all modes have less than 1% error. The lower portion of the figure displays a cross-modal assurance criterion (MAC) plot between the test and FEM elastic modeshapes. The MAC is a simple method for assessing the similarity of two mode shapes. A value of 1 indicates that the modes have the same shape, while a value of 0 is representative of completely independent shapes. When comparing large sets of modes, a matrix of values between 0 and 1 is produced, showing each modes relation to all others. Thus, the values of 1 on the diagonal represent very good agreement between the shapes. Modes 4 and 5 are likely a pair of symmetric modes, in which the FEM predicts slightly rotated lines of symmetry. Test mode 8 appears as an aliased version of mode 6.

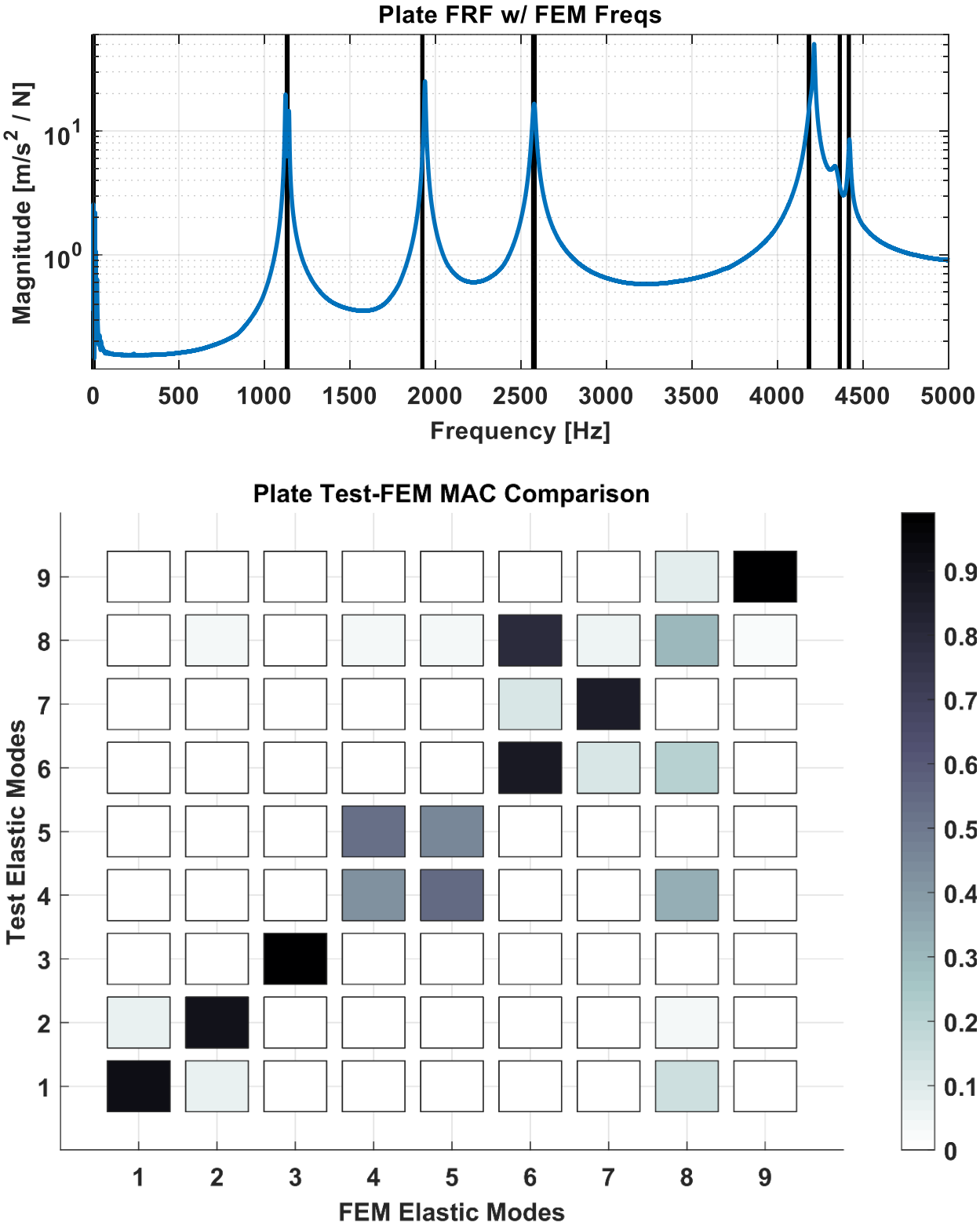

Figure 10: Plate Test-FEM Comparison (Top) Frequency and (Bottom) MAC Plot

For the plate and block FEM, Figure 11 shows the same test-FEM comparisons for frequency and modeshape. In the top of the figure, the FEM is again seen to be in very good agreement with the measured FRF, as the vertical black lines, representing the FEM frequencies, nearly pass through every peak. The largest error is less than 2%. The cross-MAC is similar to that for the plate, in that values on the diagonal are near 1, except for mode pairs 1 & 2 and 6 & 7 which are slightly rotated symmetric modes, and FEM mode 9, which did not appear in the test data.

It is of note that typical FEA solvers will produce rigid body modes that, while mutually orthogonal, are at an arbitrary orientation relative to the three unit directions of the global coordinate system. This may introduce difficulties later when selecting basis modes for the substructuring constraint equations. Thus, according to the recommended procedure [11], in this work the rigid body modes computed from the FEM were corrected so that each was purely representative of one of the six rigid body DOF. This was done by first determining the structure principle body coordinates and principle moments of inertia. The rigid body modes are then calculated by distributing the mass, for translational, or moment of inertia, for rotational, over each DOF relative to the orientation of its local coordinate system to the principle body coordinates.

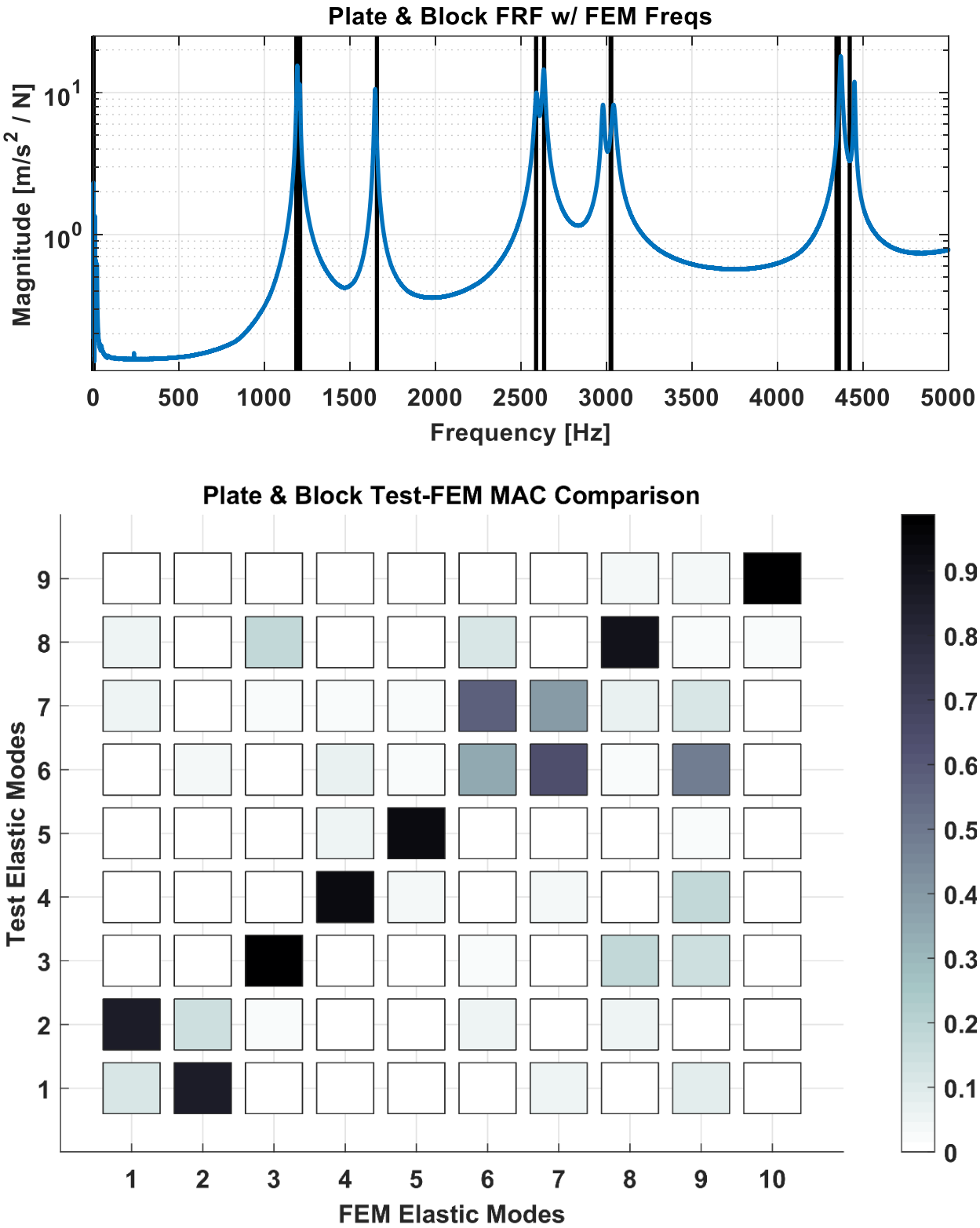

Figure 11: Plate and Block Test-FEM Comparisons (Top) Frequency and (Bottom) MAC Plot

3.4. Substructuring Results

With the experimental and FEM data collected, the TSM may be implemented as given in Eqs.(1)-(2). To define the constraint equations, a set of independent TS FEM mode shapes must be chosen as a suitable basis. The shapes must not be linearly dependent, as this would lead to ill conditioning when computing the pseudo-inverse in Eq.(2), (i.e. the amplitude of each of those basis vectors cannot be uniquely determined from the spatial information) and this would produce inaccurate results for the built-up structure. Several checks and criterion for determining a viable mode selection are given in [14, 15].

The resultant solution provides the natural frequencies and mode shapes of the hybrid structure predicted by the TSM. As the first point of comparison between these and the truth data, their cross-MAC was computed. The cross-MAC between the experimental and predicted modes of the shaker, plate & block is given in Figure 12. The string of large values on the diagonal from mode 1 to 15 is indicative of good agreement between the experimental and predicted modes. However, the nonzero off diagonal terms represent some degree of likeness between most of the modes. Also, the predicted set of modes show very little similarity to test modes 16 through 23, which corresponds to the set of small peaks visible in Figure 8 between 3000 Hz and 4000 Hz after adding the block. This indicates that the TSM model was unable to predict the creation of the group of high frequency modes.

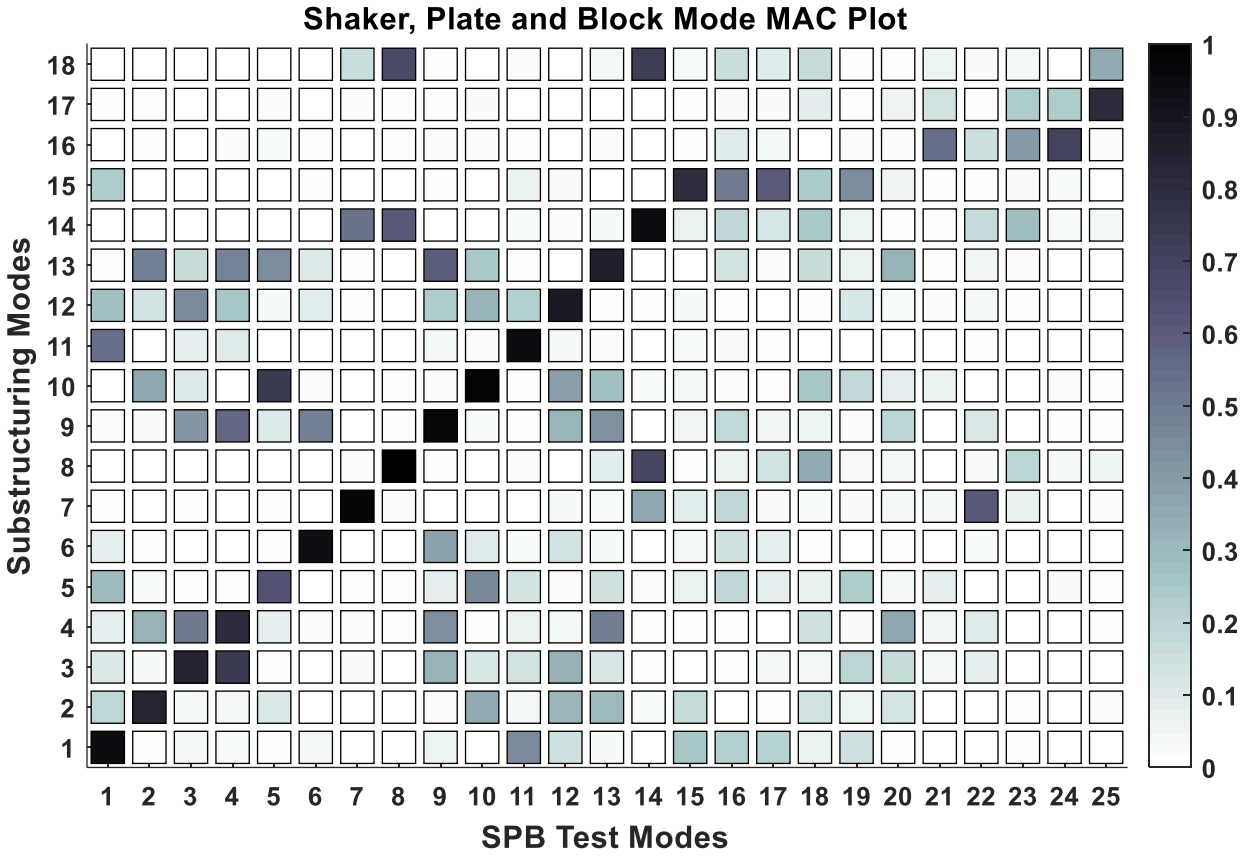

Figure 12: Cross-MAC between the Predicted and Truth SPB mode shapes

While there is good agreement between the truth data and the substructuring prediction, it was observed previously in Figure 8 that the plate and block do not significantly alter the observed shaker modeshapes. Figure 13 shows the cross-MAC between the experimentally measured modes of the shaker & plate and the shaker, plate & block, and is nearly identical to that above. This agrees with the statement that, in this case, the TSM substructuring does not need to, and is not significantly altering the modeshapes of the shaker & plate with the addition of the block. This also means that the off-diagonal terms in the MAC plots are likely due to aliasing between modes; the measurement DOF are too coarsely distributed.

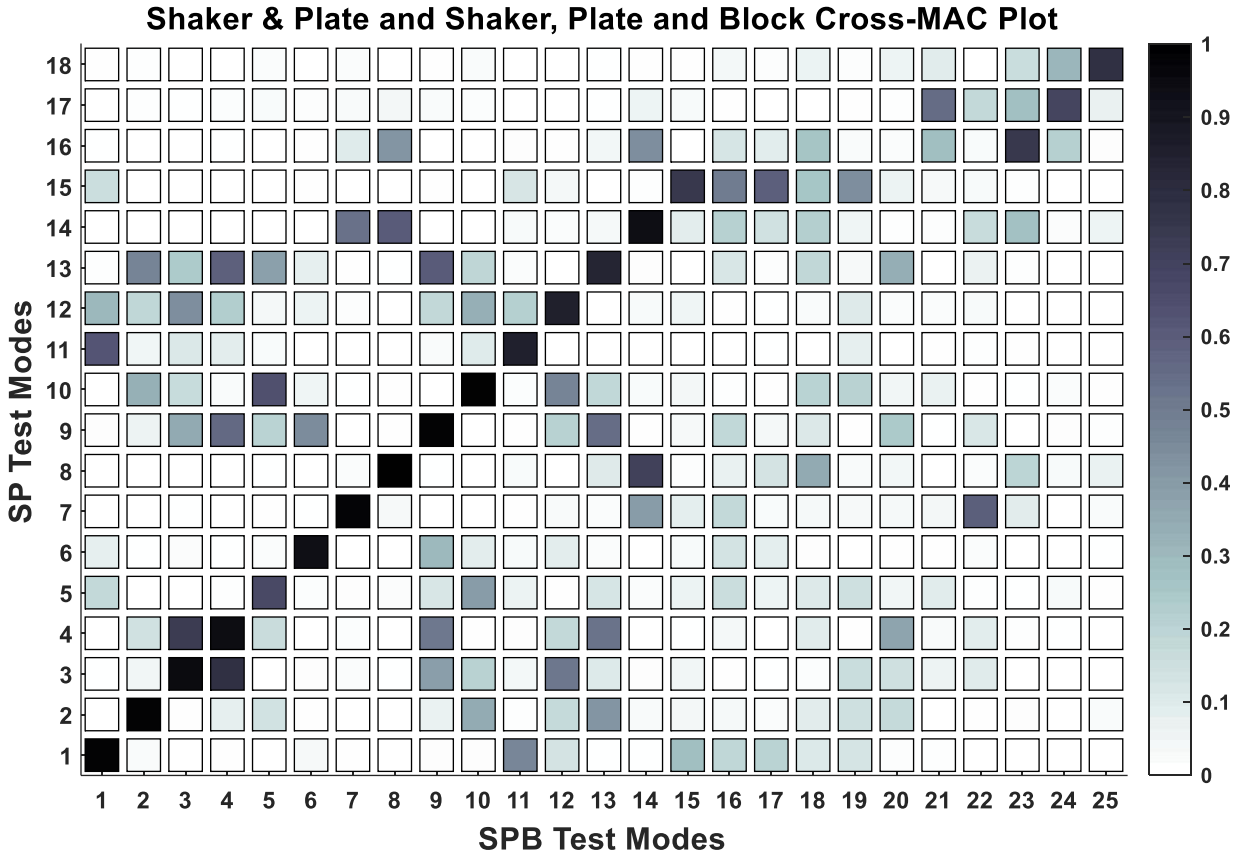

Figure 13: Cross-MAC between the SP and SPB experimental modeshapes

As a method for easily comparing the shaker model to the truth data, the substructuring results were used to generate FRFs representative of the predicted parameters. It should be noted that, as a consequence of implementing FEMs without damping data in the substructuring process, the TSM model does not predict damping ratios. Thus, to construct the FRFs, the experimental damping ratios from the shaker & plate curve fits were superimposed on the predicted mode shapes and natural frequencies. This is an assumption that the damping does not significantly change due to the presence of the block.

The results of the FRF generation and the experimental data is given in Figure 14. The yellow curve depicts the results of the TSM substructuring with the corresponding measurements from the truth test given by the red curve, the blue curve denotes the experimental measurements from the shaker and plate, which can be compared with the predicted FRFs so that the error in the substructuring predictions can be compared with the error that one would obtain if substructuring were not performed and the shaker was simply assumed to remain unchanged after adding the block. Below 2000 Hz, this would be a realistic assumption, since the only variance is a very slight decrease in natural frequency due to the additional mass of the block. However, between 2000 and 2500 Hz, the single large peak seen in the shaker & plate data splits into two peaks at significantly lower frequencies. The predicted model successfully produces this change, as seen in the zoomed plot window. The substructuring model also accurately predicts the slight change in the next peak near 2600 Hz, and the group at 4000 Hz. However, in the range between 3000 and 4000 Hz, the truth data exhibits several small peaks while the TSM model does not. This is the set of modes observed in the cross-MACs that display no similarity to the shaker & plate modes, and thus the TSM predicted shape set.

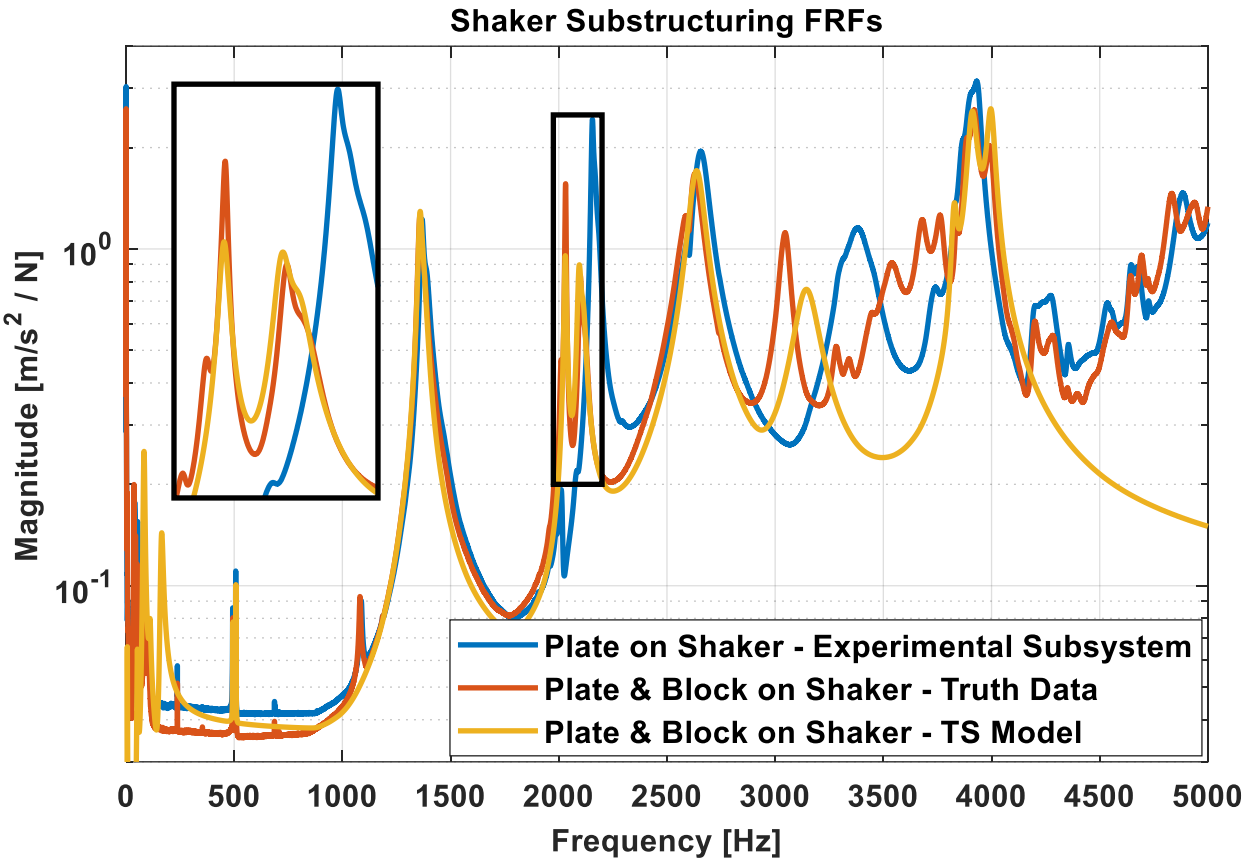

Figure 14: Comparison of experimental and predicted FRFs

Finally, as an example of how the experimentally derived model for the shaker might be used, the response of the system was calculated due to a uniform, unit force in the vertical Z direction, such as might be observed when testing a component. This was accomplished by distributing the force evenly over the Z direction drive points while zeroing the others. This was repeated for the shaker & plate and the truth and TSM predictions for the shaker, plate & block. The resultant response as a function of frequency is given in Figure 15, and can be interpreted as denoting which resonances are excited when the shaker is in operation and how much amplification is observed at each. The results show that the response is

amplified by almost two orders of magnitude near 2000 Hz, which corresponds to the first resonance of the shaker. This resonance shifts in frequency and the two close modes that comprise the peak separate when the block is attached. As was seen in the comparison of the FRFs above, the TSM model is able to predict the truth data to a reasonable degree up to about 3 kHz, although with some variance in the peak magnitudes.

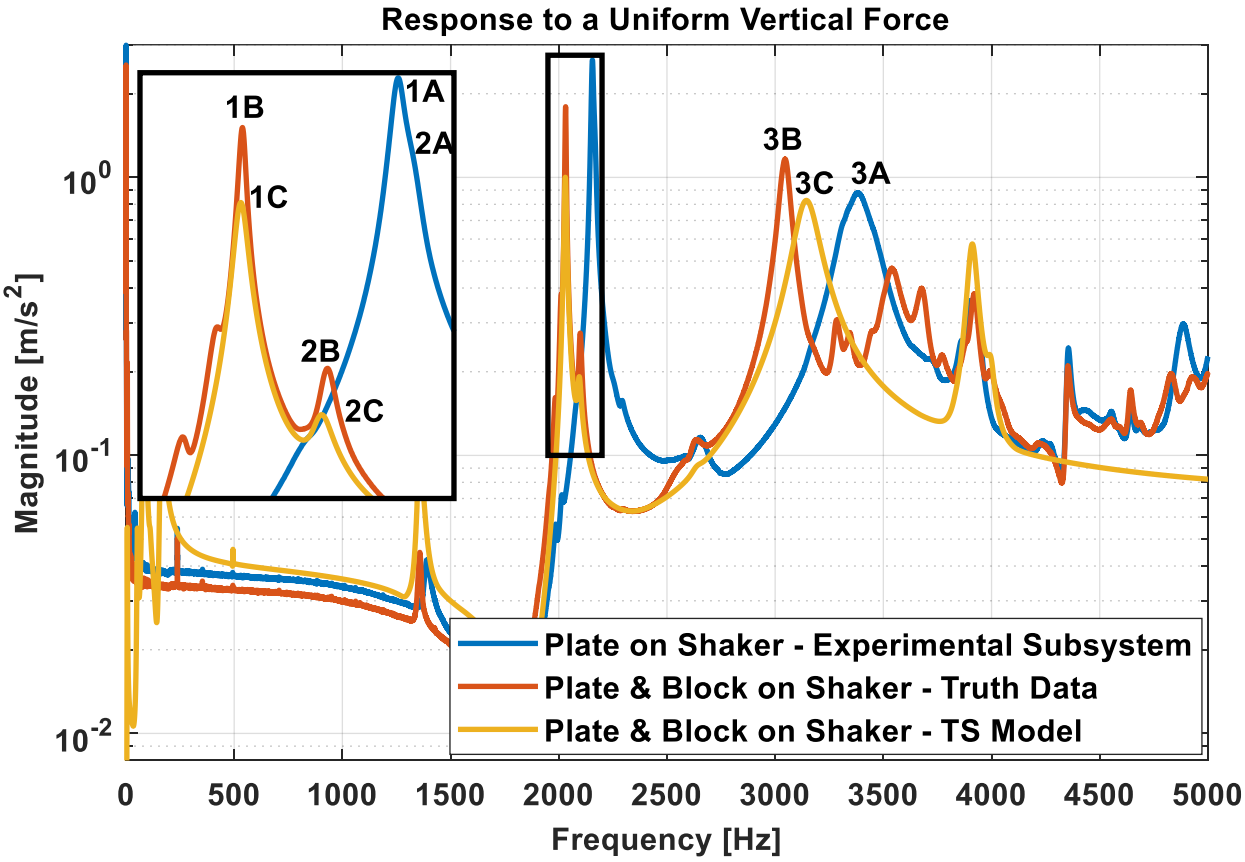

Figure 15: SPB response as a function of frequency for a uniform unit Z force

Additionally, the shape of the response at the peaks may be calculated and plotted. This provides an indication as to if certain areas of the test surface experience over or under testing when the system is at a resonance. The shapes

shown in Figure 16 are labeled relative to the alphanumeric markers denoting the peaks in Figure 15, in which each row corresponds to the shaker & plate, shaker, plate & block, and the TSM model, respectively. While it is of no surprise that all the shapes are some form of drum mode, given that a uniform Z force would highly excite these, the most interesting result is that the TSM correctly predicts the mode shape at peak 2C relative to the shape extracted from the truth data at peak 2B. This is especially notable since the mode shape of the original shaker & plate, from peak 2A, is completely different. If a test were planned based on a model of the shaker & plate (i.e. without considering how the test part would change the dynamics of the system), one might choose to locate a control accelerometer in the center of the plate, and that sensor would see very little motion as the shaker plate actually moved in a two-lobe motion with a zero near the centerline, potentially over testing any components mounted off of this centerline.

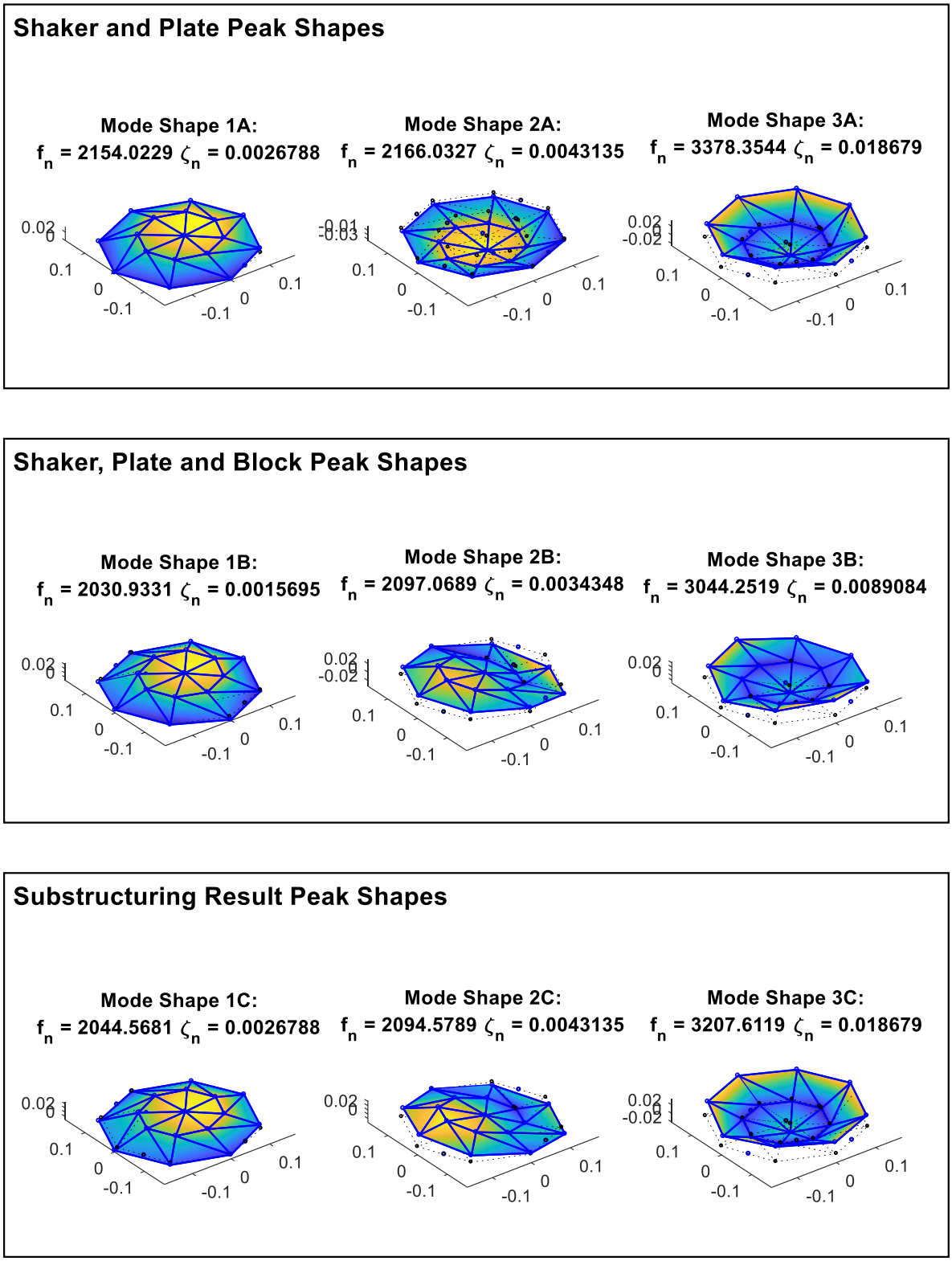

Figure 16: Peak Deformation shapes to the unit Z force

3.5. Discussion

In this test case, a simple circular aluminum plate was used as the shaker fixture, and a steel block as the test article. In testing this configuration, the response of the shaker was found to be relatively unaffected by the presence of the plate and block beyond the obvious increase in mass they contribute. This mass caused several modes past 2000 Hz to shift to lower frequencies, which the TSM was able to predict quite well. However, none of the additional small modes seen in the truth data after adding the block were created. These are possibly due to nonlinear variations in how the shaker behaves internally in response to the increase in mass on the armature. Unfortunately, this sort of change in the system is unlikely to be predicted by the TSM, as the substructuring results assume that the shaker response will be a linear variation on the initially measured experimental subsystem. That being said, the TSM was able to accurately predict all of the seemingly linear changes, i.e. the shifts in frequency due to the additional mass. While basic, this result does show that the process can work. In order to determine if equally accurate results can be achieved with a more intricate assembly, a more complex fixture and test article are needed.

4. Test Case 2: Half Cube with Beam

4.1. Subsystem Definitions

4.1.1. The Transmission Simulator

In this test case, the TS subsystem is a three-sided aluminum half cube, shown below in Figure 17. The sides are 3/4” thick, the inside dimensions make a 10” cube, and the fixture weighs approximately 21 lbs. The three sections are bolted together with thirteen 3/8” steel bolts distributed along the three seams, torqued to 37 ft-lbs. The half cube provides a plethora of attachment points for test articles and for anchoring to the shaker.

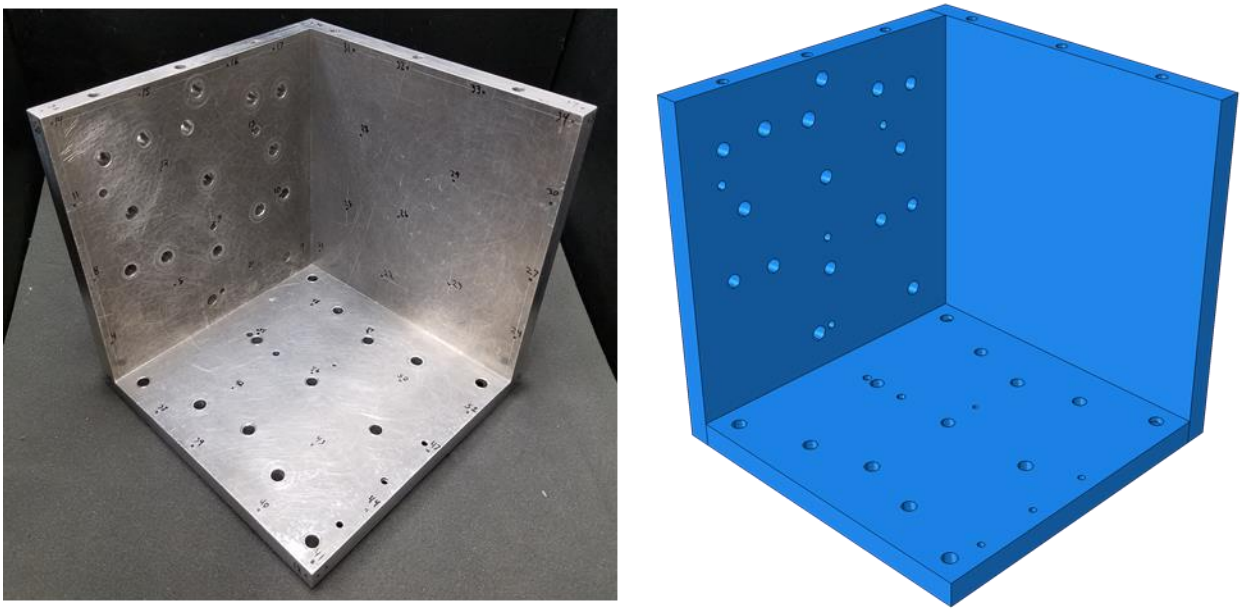

Figure 17: The Transmission Simulator. (Left) A three-piece aluminum half cube, and (Right) its CAD Model

4.1.2. Experimental Subsystem

The basis of the experimental subsystem is the same LDS V830 electromagnetic shaker from test case 1. The total subsystem, as shown in Figure 18, is the shaker with the half cube TS bolted down to the armature with nine 3/8" steel bolts torqued to 37 ft-lbs. While the bottom plate of the half cube is anchored down to the shaker in much the same way as the circular plate, similarly restricting its motion, the vertical sides are relatively free, making this configuration more dynamically challenging. A goal with this test case is to investigate how accurately the response of a complex fixture can be preserved through the decoupling and recoupling steps of the TSM.

Figure 18: (Left) The shaker system used to evaluate the proposed substructuring approach, and (Right) The Experimental Subsystem; the TS mounted on the shaker.

4.1.3. Analytical Subsystem

The analytical subsystem, the half cube with a cantilever aluminum beam, is shown in Figure 19. The beam measures 9”x1”x.25” and weighs 0.22 pounds, and is bolted and super glued to the top of the left cube plate. As opposed to the previously implemented steel block, the beam has a measurable dynamic response. An additional goal of this test case is to simulate the test article response from the model generated by the TSM.

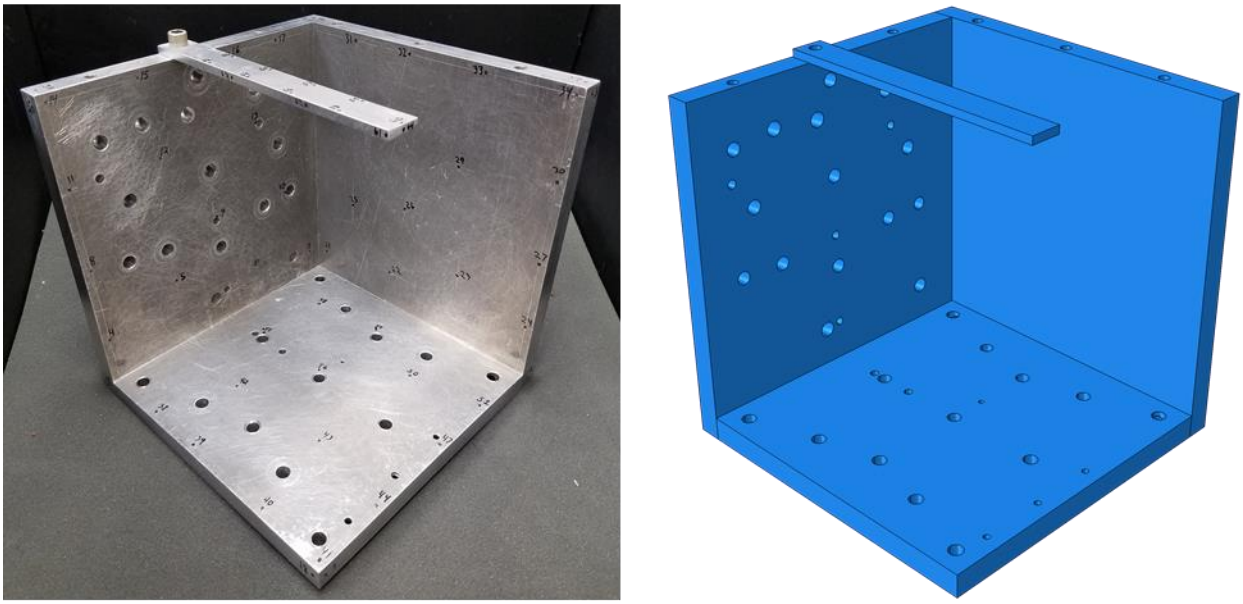

Figure 19: The Analytical Subsystem. (Left) The half cube with a cantilever beam, and (Right) its CAD Model

4.2. Finite Element Analysis

For the substructuring procedure, FEMs of the TS and the analytical subsystem were created. Again, this was done in Abaqus, resulting in the mesh shown in Figure 20. This mesh contains 350,000 nodes from 67,000 20-node hex

elements and 16,500 10-node tet elements. Complex hole geometry made an all hex element mesh unrealistic, but extensive partitioning resulted in a predominantly hex mesh with tet elements filling in around the regions with intersecting holes. Also, it is of note that bolt models in the form of simple cylinder plugs were used in prior versions of this FEM, but were found to not significantly alter the results, thus they have been omitted to reduce model complexity.

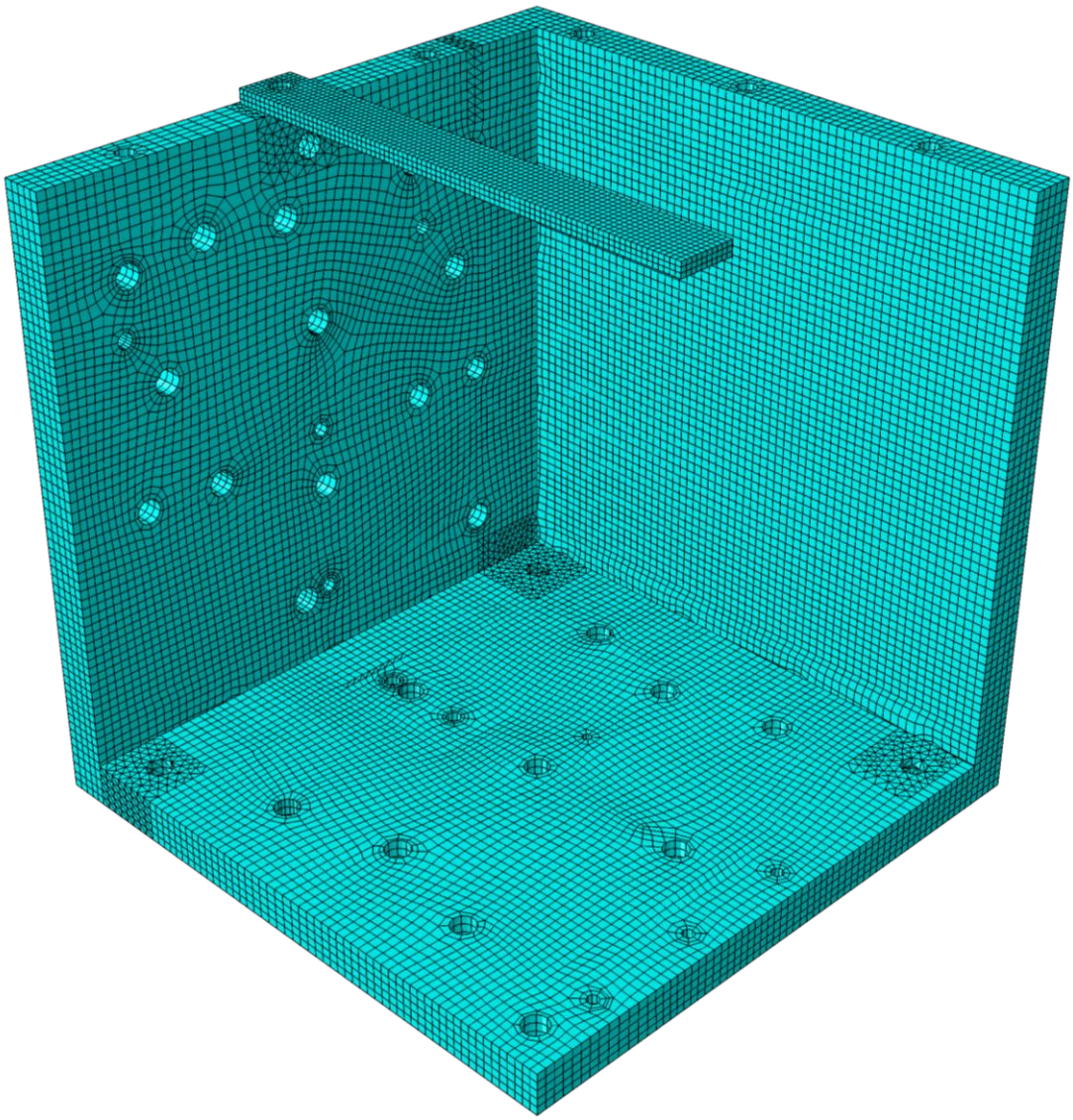

Figure 20: Finite Element Subsystem Mesh

To calibrate the baseline FEMs, natural frequencies were taken from an initial test performed on the physical half cube in which a modal hammer was used to strike the half cube once near the free corner on each of the three sides. Material properties, including elastic modulus and Poisson's ratio, were tuned via a guess and check method until good agreement was found between test and FEM frequencies. Final values of 1e7 psi for elastic modulus and 0.33 for Poisson's ratio were found. An average density of 0.1 lb/in^3 was set from mass values measured from the physical components. Also, a point mass of 0.03 lbs was added to the beam tip to account for the accelerometer weight.

The contact between the aluminum plates was also optimized. This involved varying the size of a bonded contact area around each bolt hole. The final contact areas, shown below in Figure 21, extend approximately ½" to either side of the bolt holes. Setting the open area between bonded zones to various states of contact was found to only degrade results, thus these zones were left free of a defined contact property.

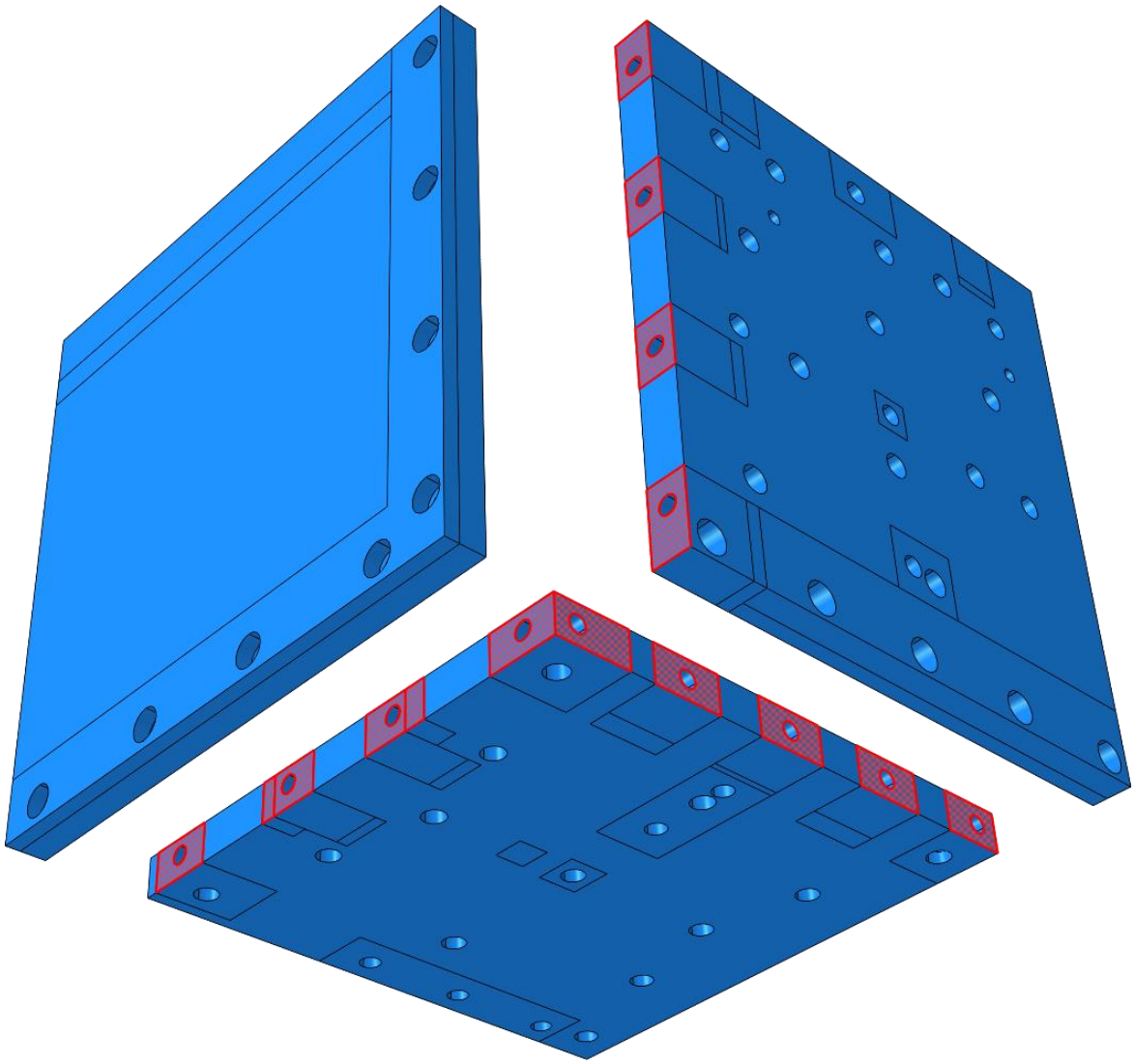

Figure 21: Bonded contact areas defined in the FEM

4.3. Experimental Setup

An experimental modal model for the experimental subsystem, the TS mounted on top the shaker, was created by conducting a roving modal hammer test of the structure. The location and direction of each hammer hit are shown below in Figure 22. The coordinates and direction of this set of points was selected with

Effective Independence [16]. This is a process through which an initial large set of potential test points from a FEM are iteratively reduced based upon preserving the information contained in a set of target modeshapes. From an initial set of approximately 4000 points from the FEM in Figure 20, the set of 51 points on the half cube and 13 points on the beam were produced to capture the first 35 modes of the system, which extends to 6500 Hz.

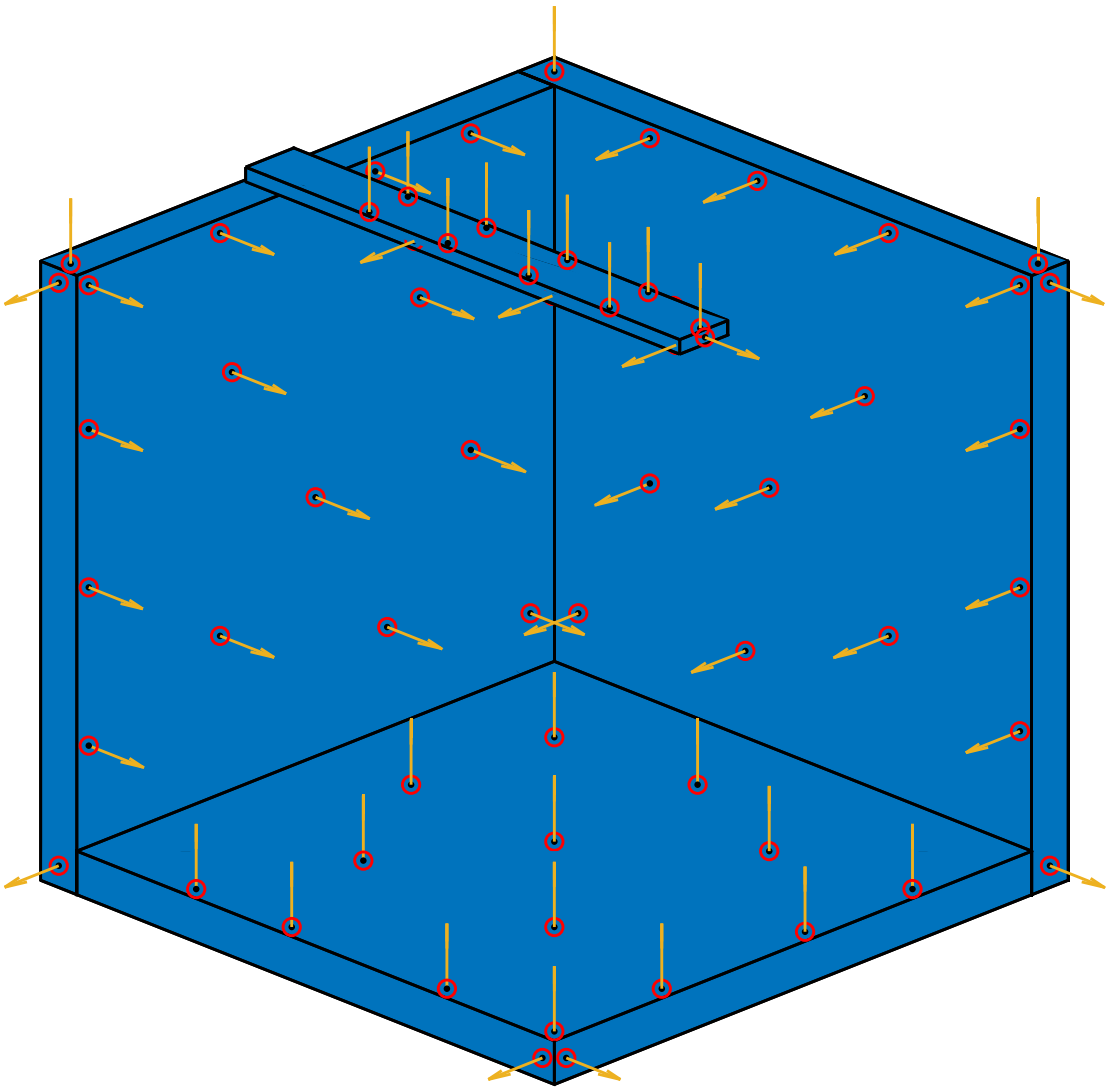

Figure 22: Roving hammer hit locations and directions from Effective Independence

The accelerometer responses were again recorded in Data Physics SignalCalc® 830 using the Data Physics Abacus® frontend (Figure 23). A frequency span of 0 - 10,000 Hz was set to capture enough modes of the experimental subsystem to produce accurate substructuring results for the operable range of the shaker, as modes out to twice the target range are typically needed [11].

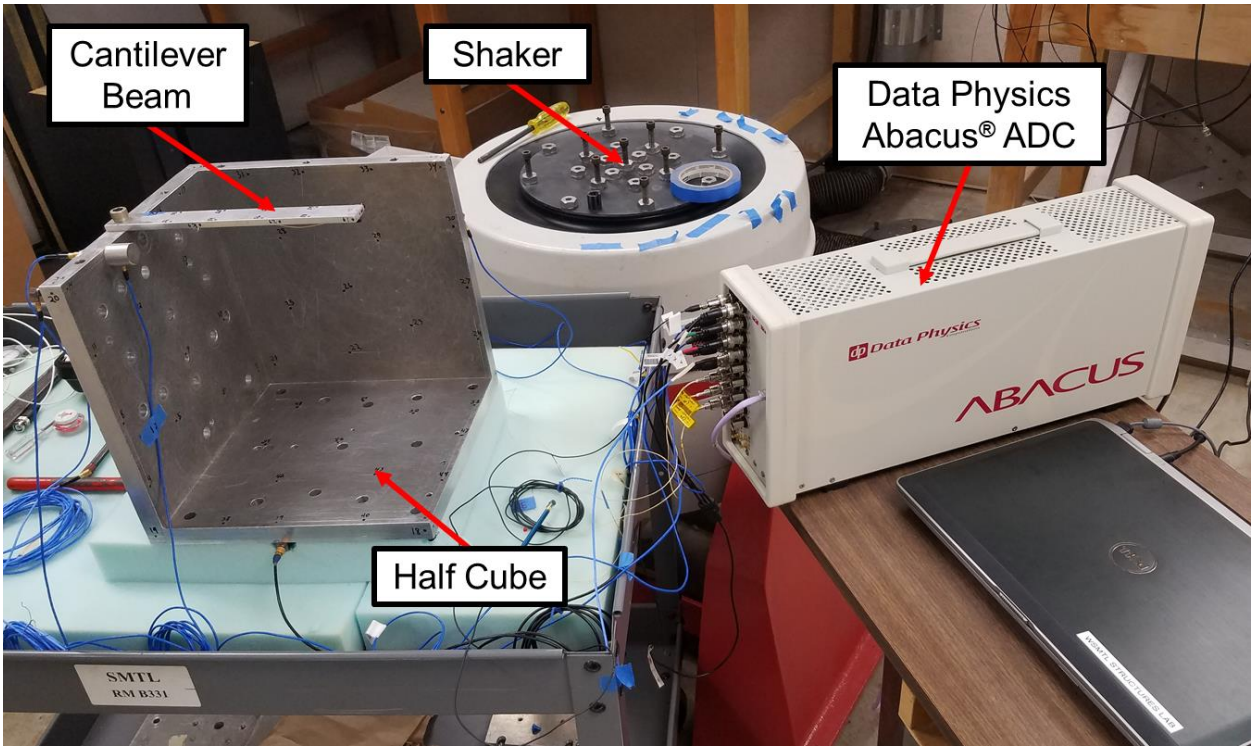

Figure 23: Instrumentation for experimental data acquisition

A roving modal hammer test was performed on each of the following: the half cube isolated on foam, the half cube and the cantilever beam on foam, the half cube attached to the shaker, and the half cube and beam attached to the shaker. The first two tests simulate free boundary conditions, providing data to further validate the FEMs. The third test is the only one that would be strictly necessary in the

application of interest and is used to create an experimental model of the shaker and half cube. The final test provides truth data, allowing assessments to be made on how well substructuring has worked in this application. A summary of the results from these test cases is shown in Figure 24.

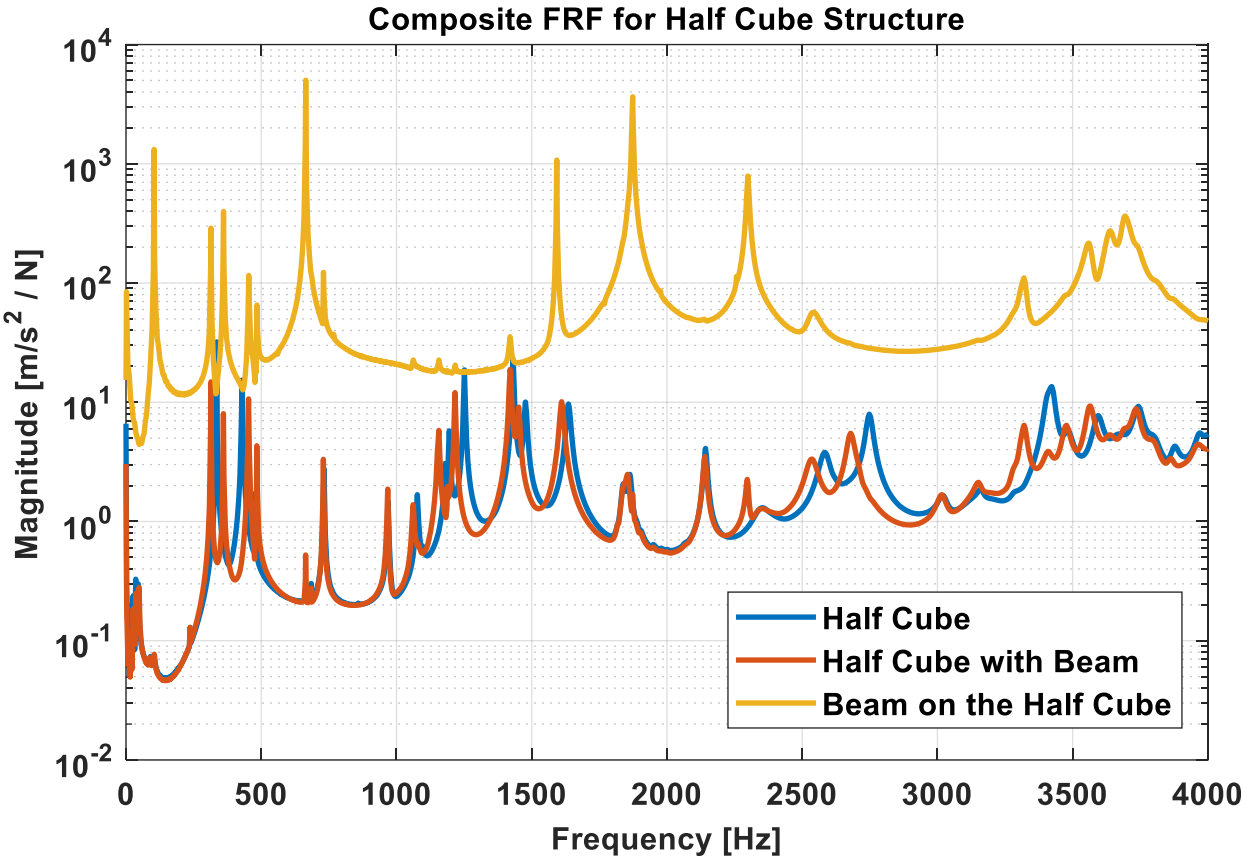

Figure 24: Average FRFs from the free tests of the TS and FE subsystems

The blue curve provides a composite of all FRFs from the isolated half cube, or the transmission simulator. To facilitate comparison, the FRFs from the beam plus half cube are divided into two parts. The orange curve shows the composite of the measurement points that are on the half cube, while the yellow curve shows the measurements from the beam. It can be seen that the response of the cube does

not drastically change due to the presence of the beam. This is expected given the size and mass difference between the two components. As a result of this, it is expected that substructuring should predict the slight changes observed on the transmission simulator, but mainly preserve its dynamics. The beam measurements show that several beam modes are within the target frequency range of the shaker and should be captured in the final assembly. Curve fitting for the experimental data was again done using AMI.

To validate the FEMs, the natural frequencies and modeshapes of each were compared to their experimental counterparts. For the TS, or the half cube isolated on foam, the comparisons are shown below in Figure 25. In the top portion, the composite FRF of all the test points is given as the blue curve. The black vertical lines represent the FEM natural frequencies. There is very good agreement through 6500 Hz. The lower portion displays a Modal Assurance Criterion (MAC) plot, comparing the test and FEM modeshapes. This shows that the first 29 elastic test modes very closely correspond to FEM modes. These are the same modes whose frequencies corresponded closely in the upper plot. Also, these modes correspond perfectly to the target set of modes defined within Effective Independence when the test locations were chosen.

The comparison for the half cube with the beam, or the analytical subsystem, is shown in Figure 26. As with the TS, the FEM for the analytical subsystem agrees well in frequency and modeshape within the first ~6500 Hz.

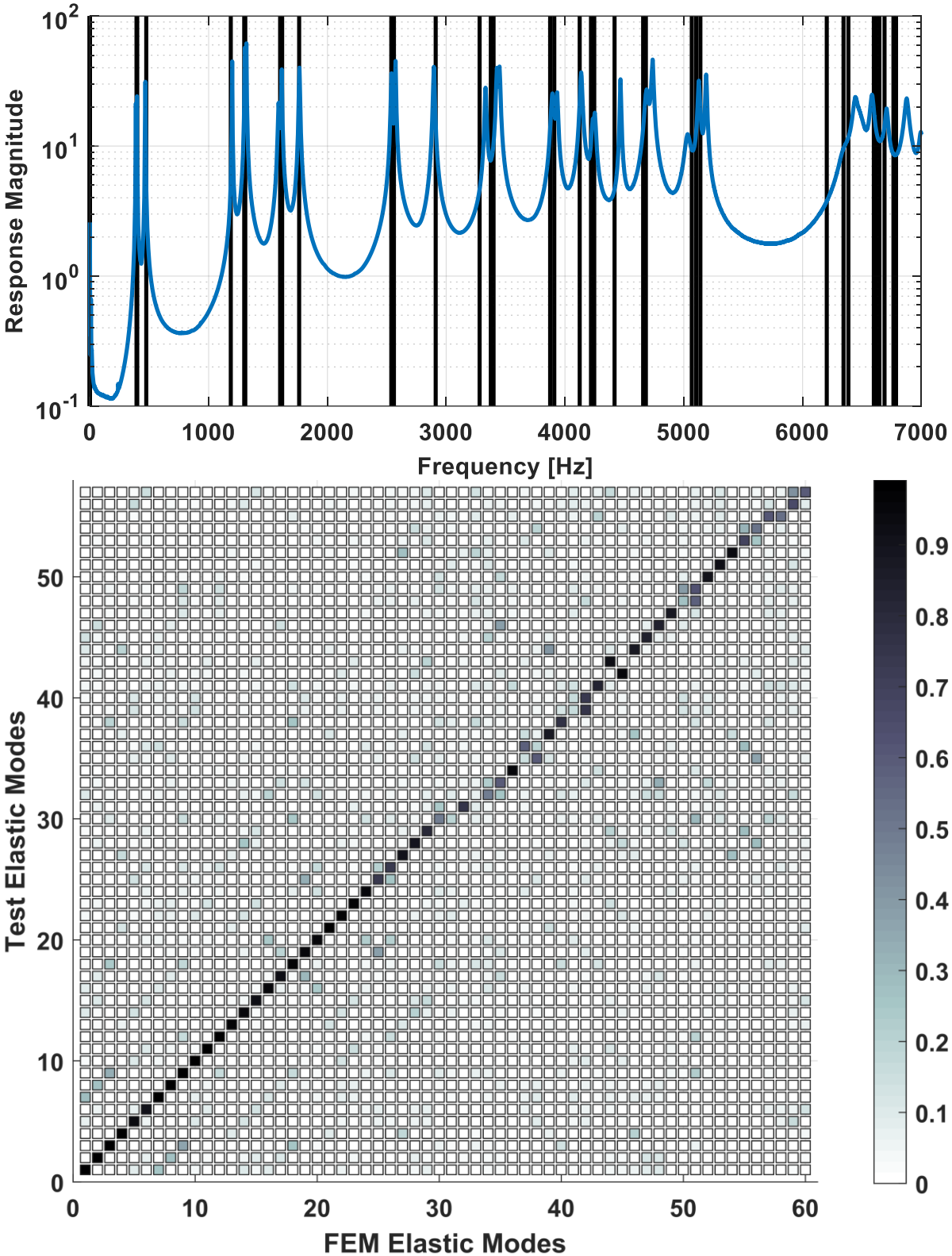

Figure 25: TS Test vs FEM - (Top) Natural Frequency, and (Bottom) MAC Plot

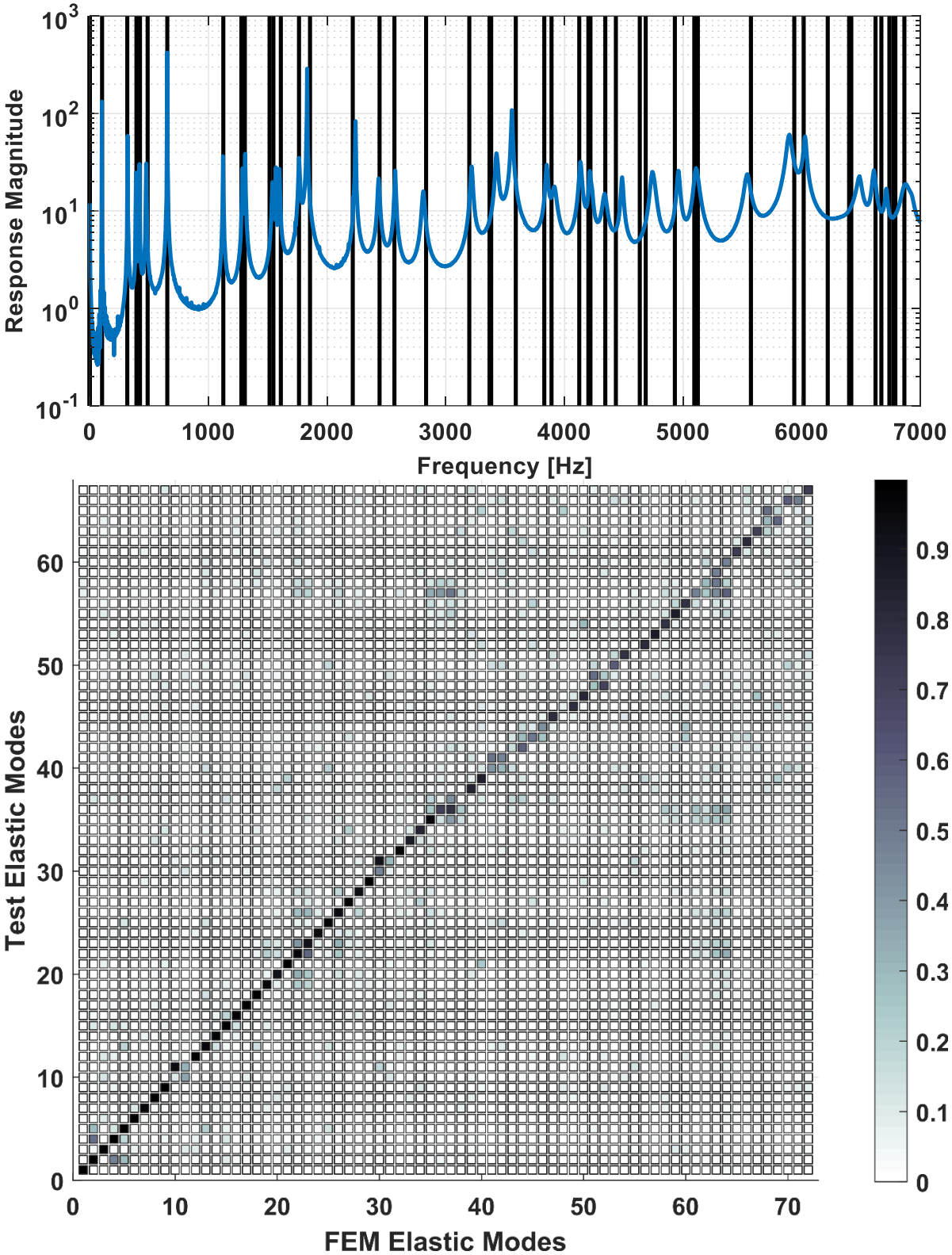

Figure 26: Analytical Subsystem Test vs FEM - (Top) Natural Frequency, and (Bottom) MAC Plot

4.4. Substructuring Results

With the necessary modal data collected for each subsystem, the TSM may be applied as given in Eqs. (1)-(2). It is of note that, to define the constraint equations, a suitable basis of linearly independent TS FEM modeshapes must be chosen. If linearly dependent shapes are included, the pseudo-inverse in Eq. (2) becomes ill conditioned and an insufficient number of constraints are enforced to satisfy the coupling equations of motion, resulting in wildly inaccurate predictions for the assembled structure. Reference [14] provides several checks and criterion for determining a viable mode selection. In the current work, the first 54 modes of the experimental subsystem were used, spanning from 0-5000 Hz. For the TS, the first 35 modes were used, which corresponds to the number of FEM modes up to 6500 Hz. These were the FEM modes of the TS that were found above to agree very well with experiment. The analytical subsystem (TS plus beam) was represented by its first 48 modes, which spans 0-6700 Hz. This was chosen so that the TS and analytical models were roughly removing and then adding the same range of dynamic information.

The resultant natural frequencies and mode shapes of the hybrid structure predicted by the TSM were used to reconstruct drive point FRFs for easy visual comparison with the truth data. It should be noted that, for this work, damping was not accounted for in the FEMs, and thus zero damping is predicted. For the FRF reconstruction, a damping ratio of .25% was applied to all modes. Figure 27 shows a comparison between the predicted and truth drive point FRFs at the tip of the beam

in the vertical direction. The transmission simulator method has successfully transferred in the first three cantilever beam modes in this direction, as given by the three large modal peaks in the FRFs. These predicted modes are quite accurate with respect to frequency out to around 3000 Hz, after which the results vaguely resemble the truth data, but are inaccurate.

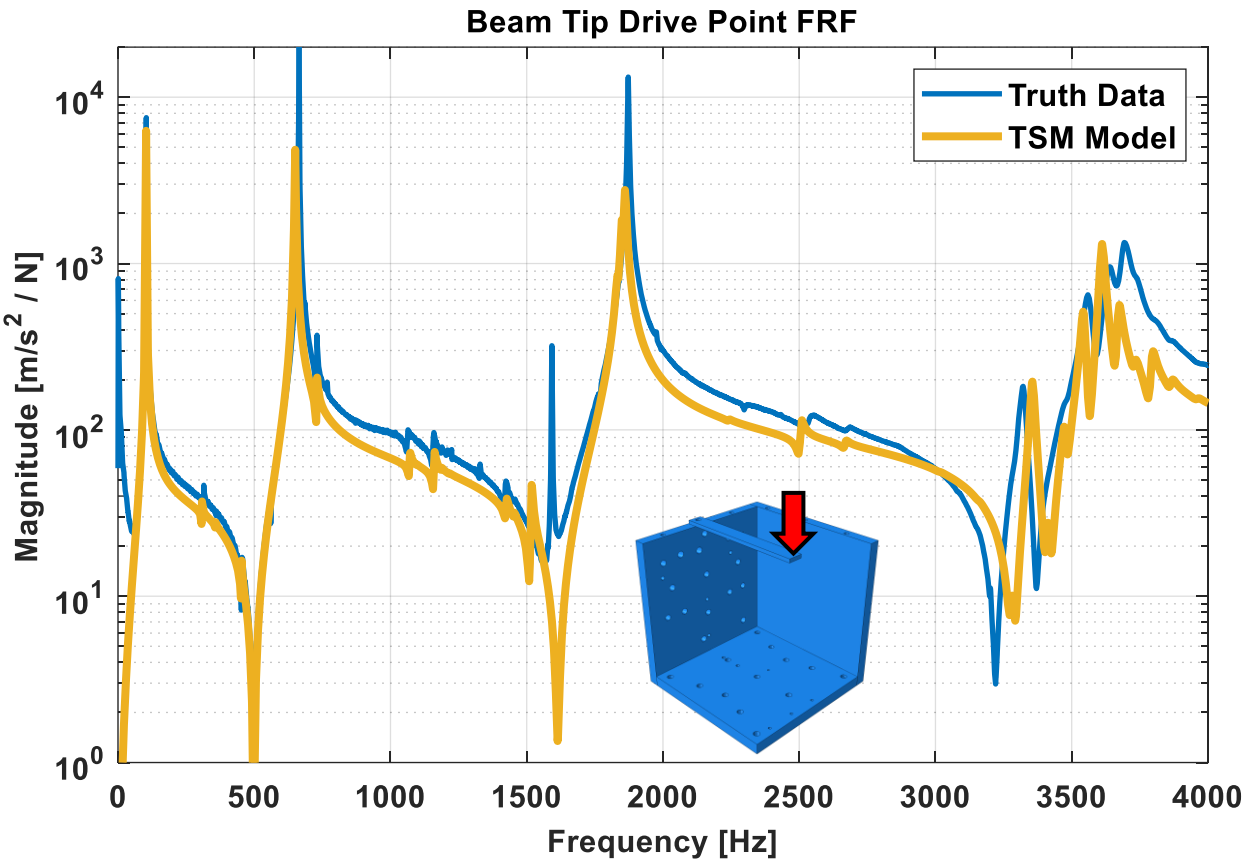

Figure 27: Prediction vs. Truth for vertical drive point FRF at the beam tip

Figure 28 shows the predicted and truth drive point FRFs at the top left corner of the half cube, next to the beam. As with the beam tip, the prediction is quite accurate and is in good agreement with the truth data. The results again become somewhat less accurate past 2500 Hz. This shows that the dynamics of the half

cube were successfully preserved through the substructuring process and that complex transmission simulators can be handled quite effectively.

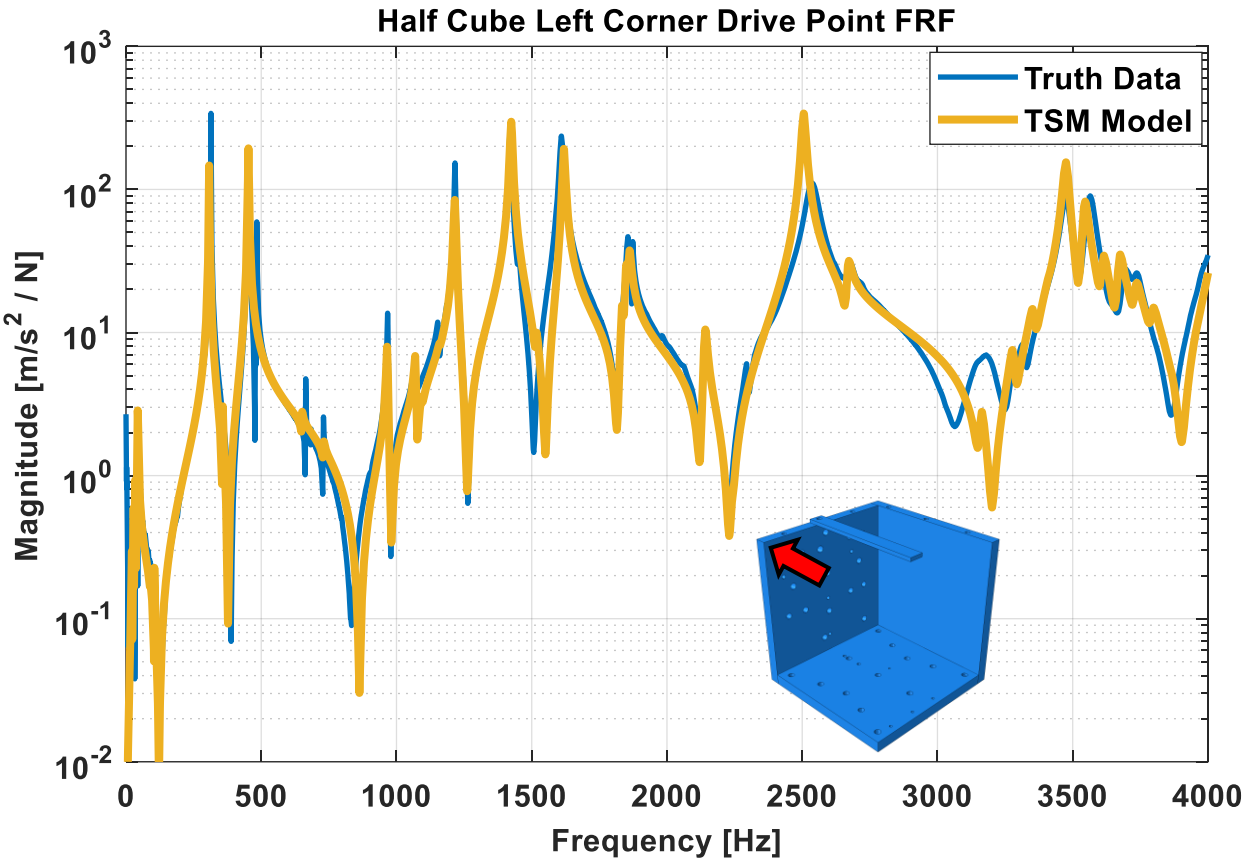

Figure 28: Prediction vs. Truth drive point FRF at the top left corner of the half cube

4.5. Discussion

In this test case, the framework developed in test case 1 for implementing the TSM on an electrodynamic shaker has been applied to a system containing a more complex fixture. It was shown that a cantilever beam, representing a mock test article, could be assembled onto a relatively complicated half cube shaker fixture, the TS, while preserving the dynamics of the half cube in the process. This was

possible due in part to the optimal test point locations chosen with Effective Independence. This allowed there to be an adequate number of modes in each subsystem basis set to achieve quite accurate results past 3000 Hz. Test case 1 likely suffered because the test locations were chosen somewhat arbitrarily, leading to relatively more difficulty in selecting a basis set than the current test case.

While this test case achieved the goals of preserving the half cube dynamics while including the cantilever beam, the beam did not significantly impact the dynamics of the assembly as a real test article might. Evaluating an additional test case in which the test article alters the dynamics of the fixture would further support the reliability of modeling an electrodynamic shaker with the TSM by demonstrating a more arbitrary testing scenario.

5. Test Case 3: Half Cube with Block

5.1. Subsystem Definitions

In this final test case, the TS and experimental subsystems are the same as those implemented in test case 2, or the aluminum half cube shown in Figure 17 and the half cube mounted on the shaker as shown in Figure 18. The analytical subsystem is now as shown in Figure 29, in which the half cube TS has the steel block from test case 1 bolted to its left side. The additional mass provided by the block warps the dynamics of the half cube, making the coupling and uncoupling steps of the TSM more challenging. And, while the block will not display any real dynamic response of its own, the assembly response at its surface can be compared to experimental measurements.

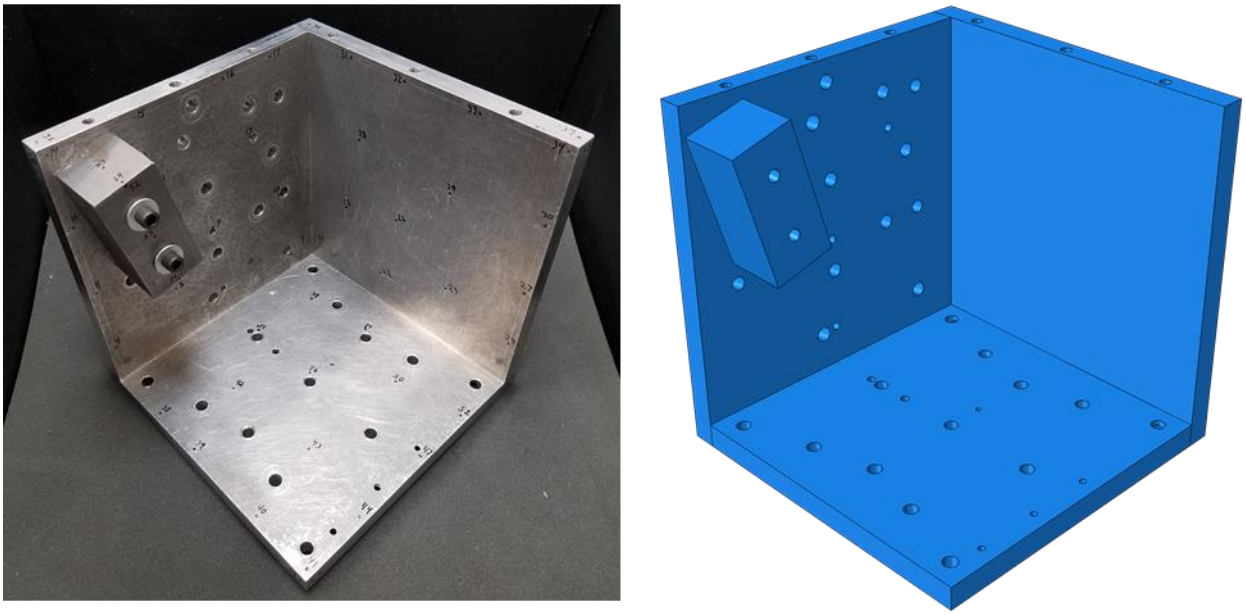

Figure 29: Analytical Subsystem, (Left) the half cube with an attached steel block, and (Right) its CAD model

5.2. Experimental Setup

For this test case, the same hammer and accelerometer layout was implemented as that used in test case 2, with the exception of a triaxial accelerometer placed on the face of the block and several hammer hits on each block face as seen in Figure 30.

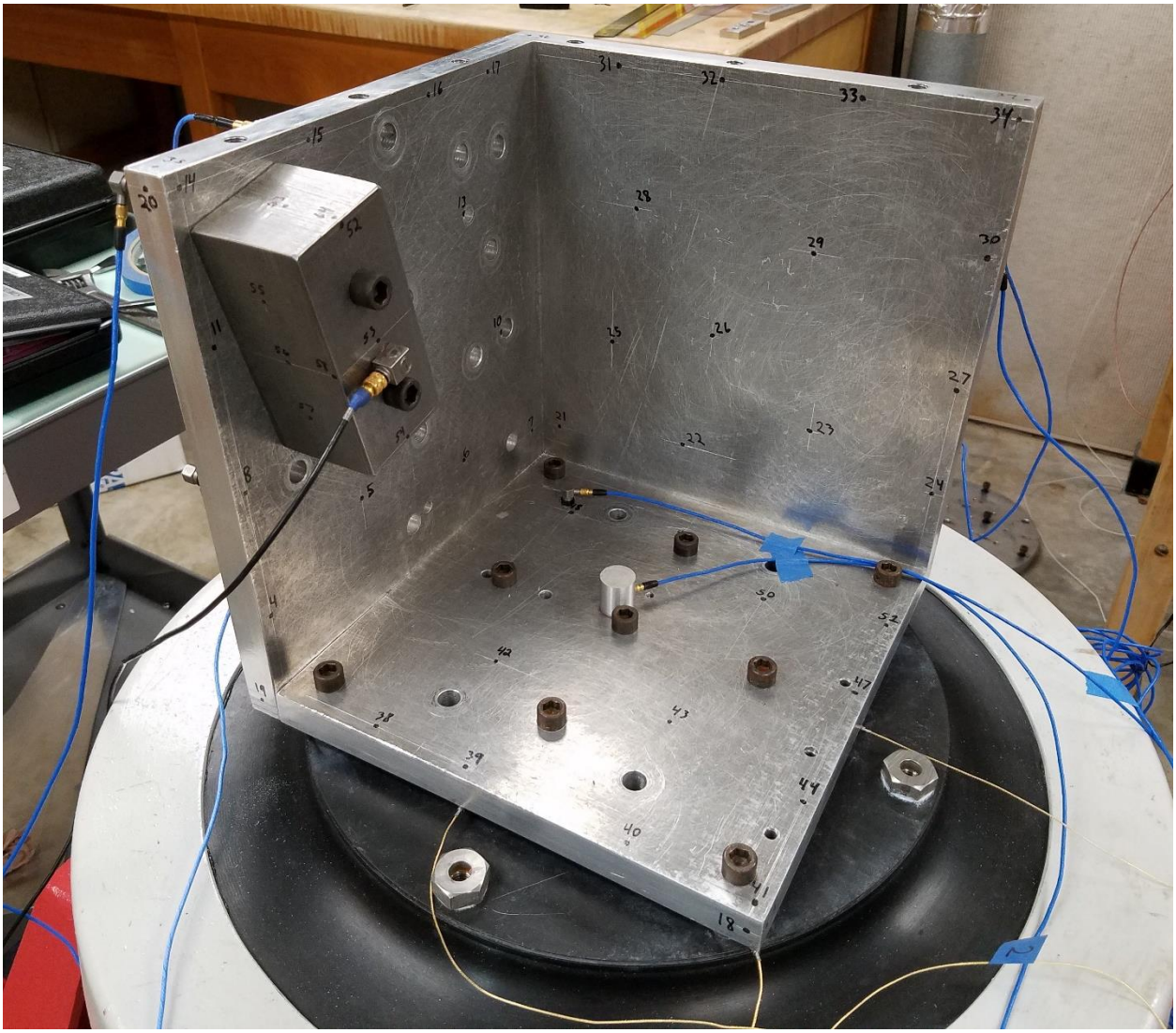

Figure 30: Half cube with block test setup

The composite FRFs from the on-shaker modal hammer testing of the half cube with and without the steel block are shown in Figure 31. The addition of the block results in a general decrease in natural frequency that mixes and blurs the ordering of the modes. This is the intended effect, as the block mass loads a single side of the half cube, biasing the overall dynamics of the system.

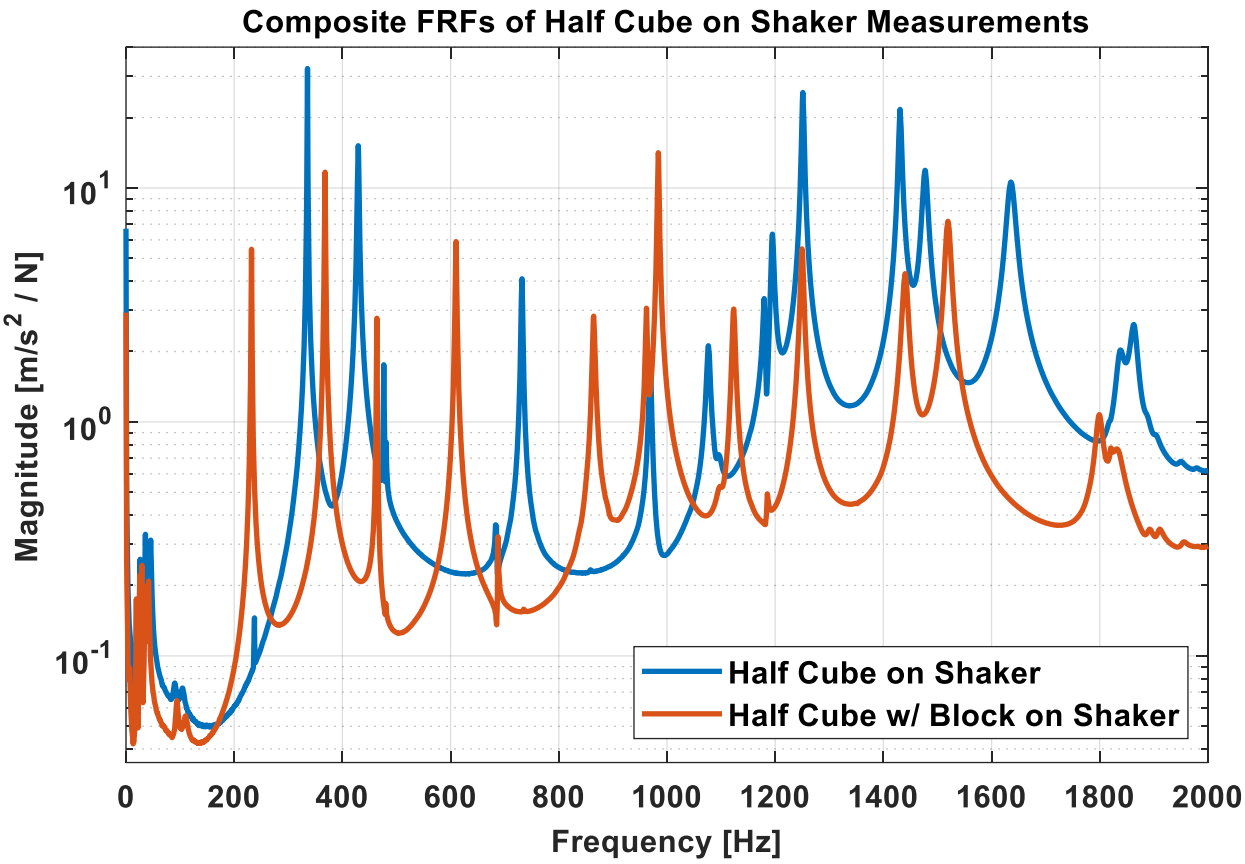

Figure 31: Comparison of half cube composite FRFs with and without the block on the shaker

5.3. Finite Element Analysis

The analytical subsystem FEM model for this test case essentially combines the half cube FEM from test case 2 with the block FEM from test case 1. The contact

definition between the block and the cube is defined as bonded except for the outer .25” around the outer edge of the block, which has no defined contact.

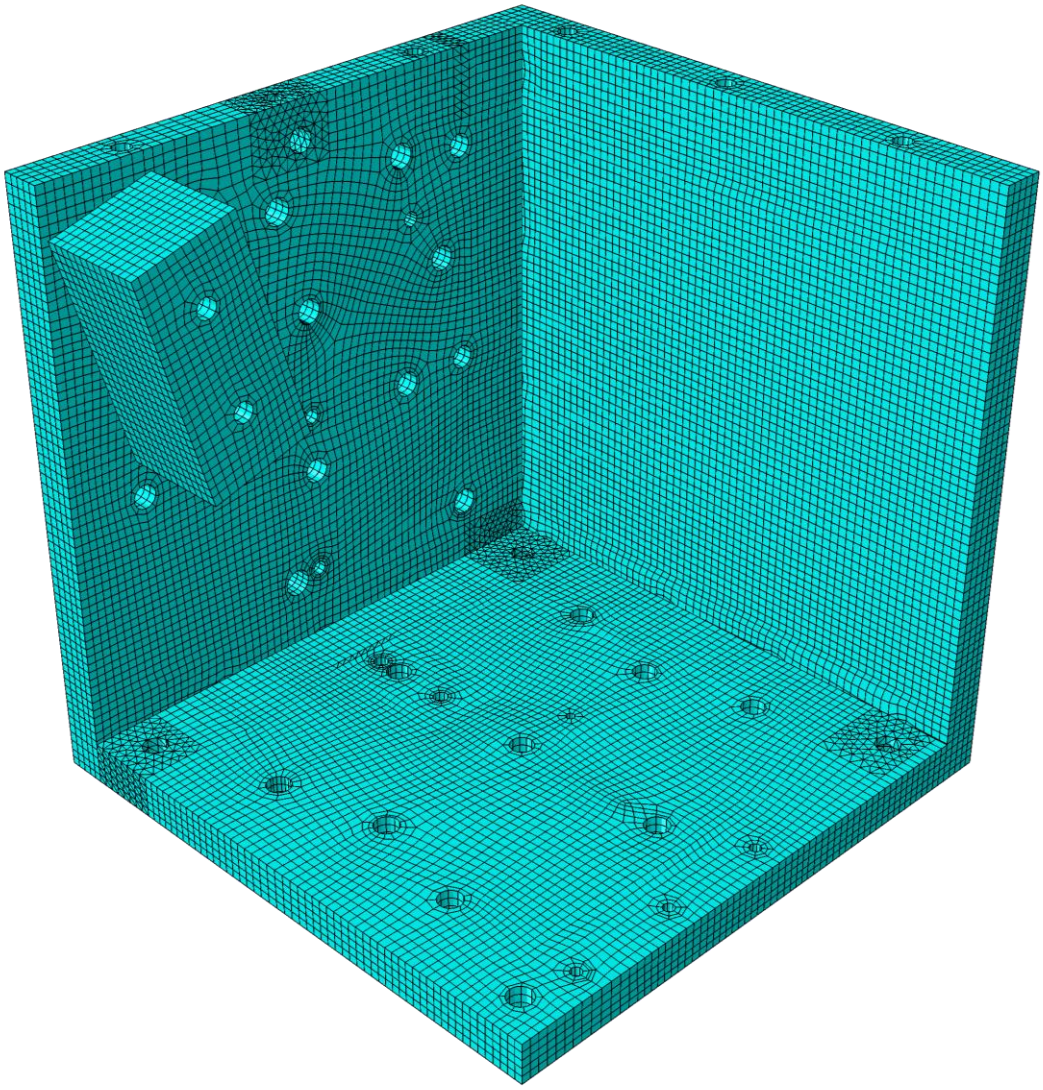

Figure 32: Analytical Subsystem FEM, half cube and steel block

This produces a model that agrees well with the on-foam experimental results, as shown in Figure 33. As previously, the top portion compares natural frequency, with the vertical black lines matching well with FRF peaks. The MAC plot in the bottom portion shows good correlation through nearly the entire test range.

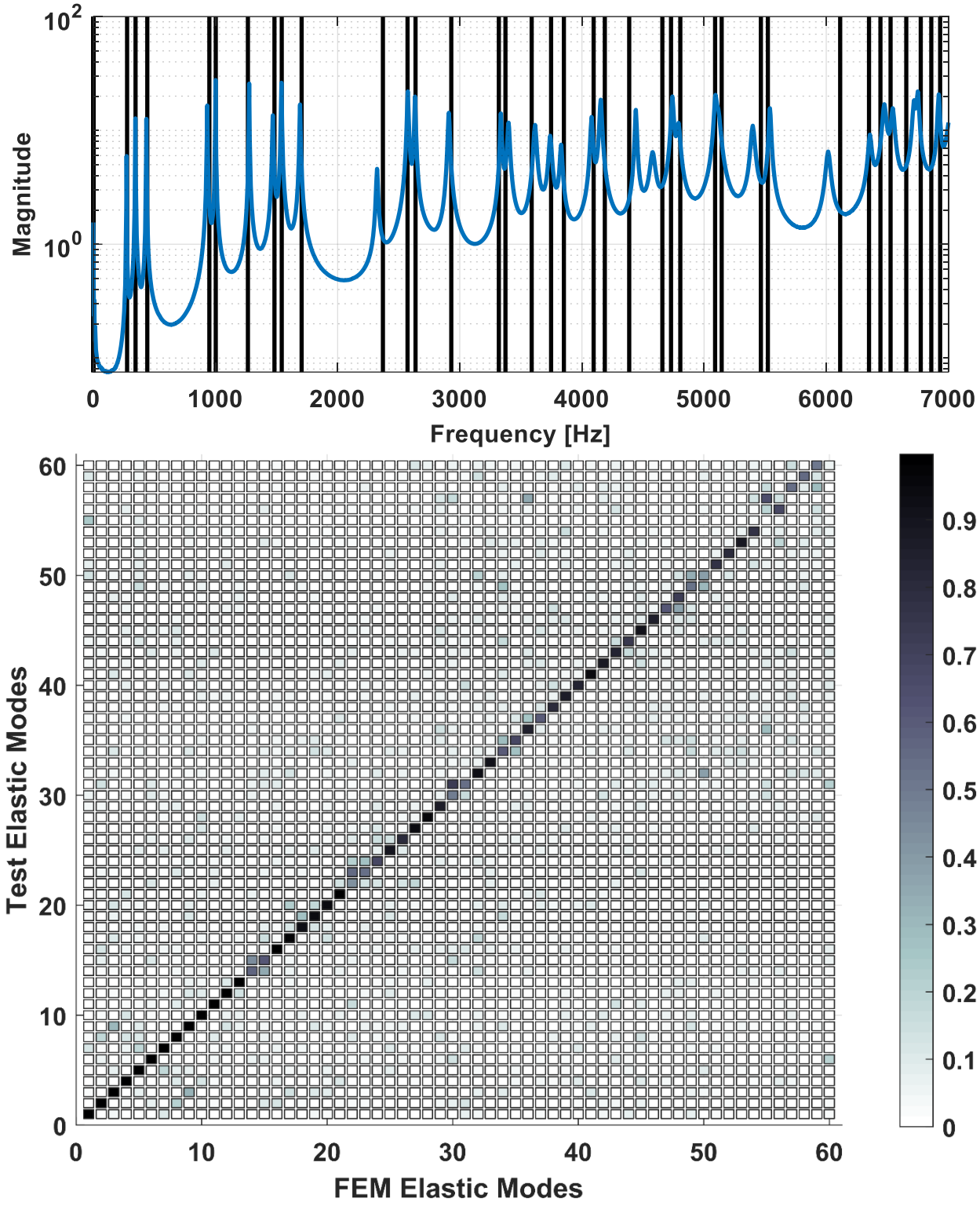

Figure 33: Analytical Subsystem Test vs FEM - (Top) Natural Frequency, and (Bottom) MAC Plot

5.4. Substructuring Results

For this test case, the process implemented in test case 2 was simply altered to use the new analytical subsystem in place of the half cube and beam FEM. It was found that for the TS, the first 44 modes could be used, reaching out to 7200 Hz. The analytical subsystem is then represented by its first 50 modes, spanning 7750 Hz. The experimental subsystem, the experimental modes of the half cube on the shaker, used the full set of measurements taken, up to 10,000 Hz. It is of note that this range extends further than the basis sets used in test case 2, possibly due to the analytical subsystem FEM showing good agreement with test out to nearly 10,000 Hz.

To evaluate the model produced by the TSM, FRFs were reconstructed at several locations. The first, depicted in Figure 34, shows a drive point FRF at the top right corner of the half cube, as marked in the figure. The three curves represent the truth data in blue, the original experimental subsystem data in orange, and the TSM model in yellow. It can be seen that the TSM model agrees with the truth data quite well through the frequency range shown. However, when compared to the original experimental data of the half cube on the shaker, adding the block does not significantly alter the response. This is not completely unexpected, given that the block is located on the opposite side of the cube and likely has a limited effect on this drive point.

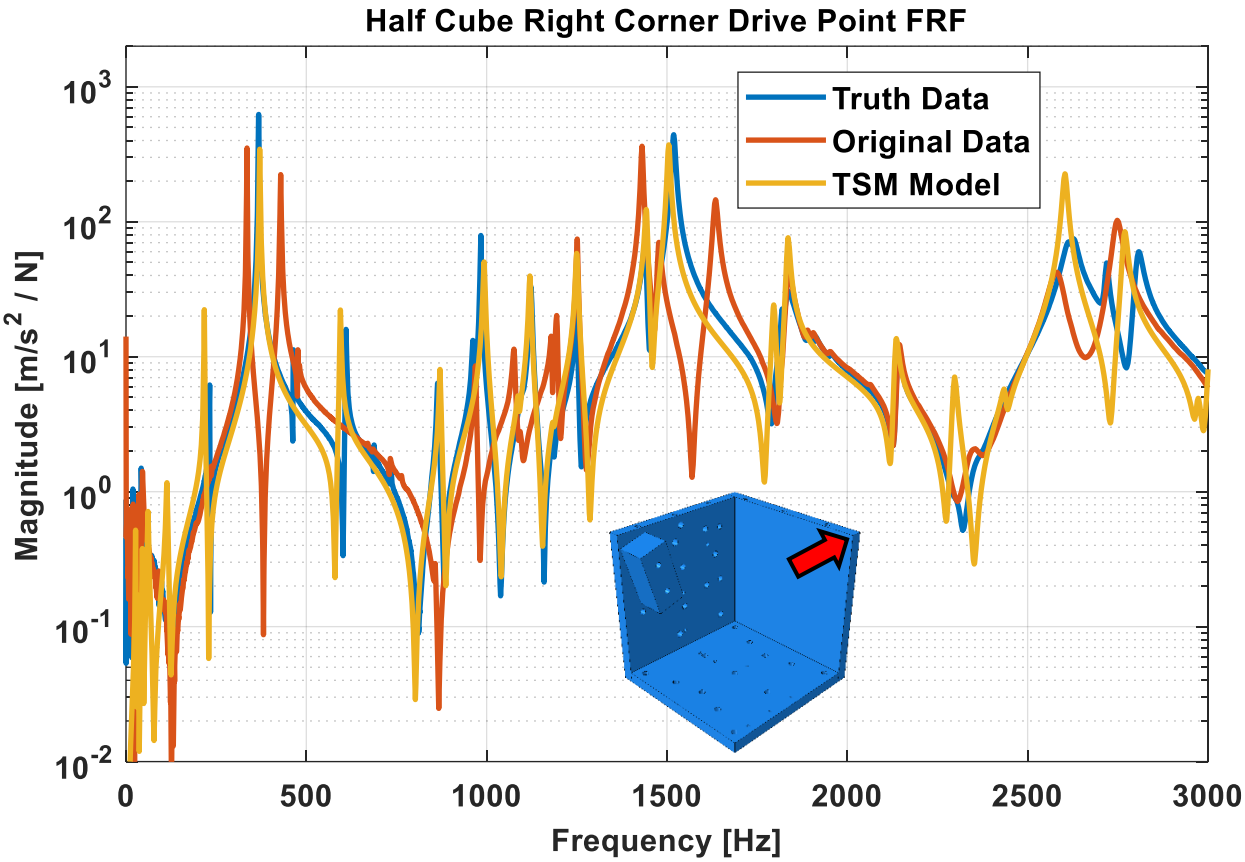

Figure 34: Half Cube top right corner FRF comparison

To verify the response near the block, the drive point on the top left corner of the half cube, directly above the block, is compared in Figure 35. As in the previous figure, the truth data, original experimental subsystem data, and the TSM model are given. However, unlike the previous drive point, the response here is drastically different when the block is present. The TSM manages to predict the altered response quite closely up to 1500 Hz, after which the model only very roughly follows the truth data.

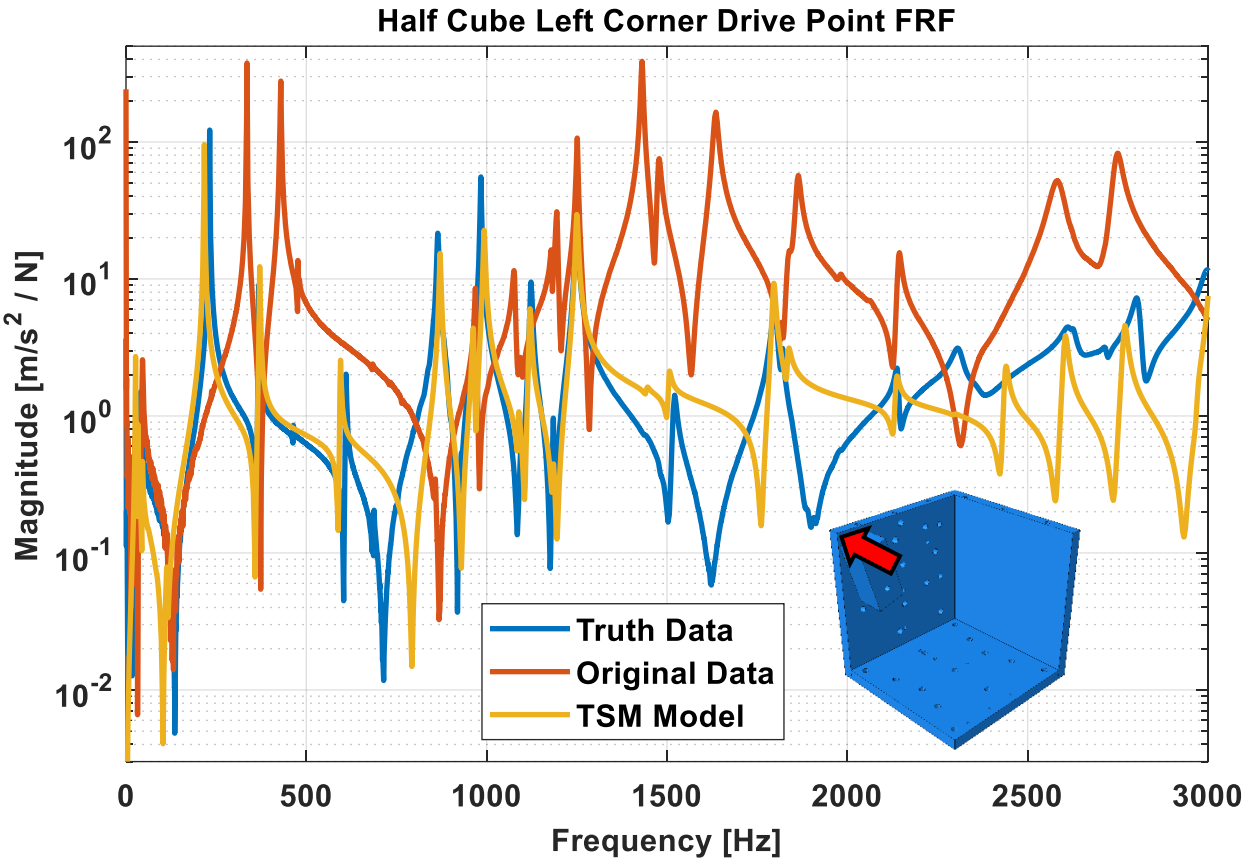

Figure 35: Half Cube top left corner FRF comparison

Thus far, the TSM models have been compared to drive point FRFs from modal hammer testing. While useful for checking the validity of the model, this is not entirely representative of the actual purpose of the model; to simulate the response of the system during a shaker test. While the block itself does not show any dynamic response in the frequency range of interest here, the response of the assembly in the vertical direction at the surface of the block can be computed and compared to measured truth data from a sine sweep of the shaker. This is shown in Figure 36, where the reconstructed TSM model FRF matches the measured response reasonably well up to approximately 1300 Hz.

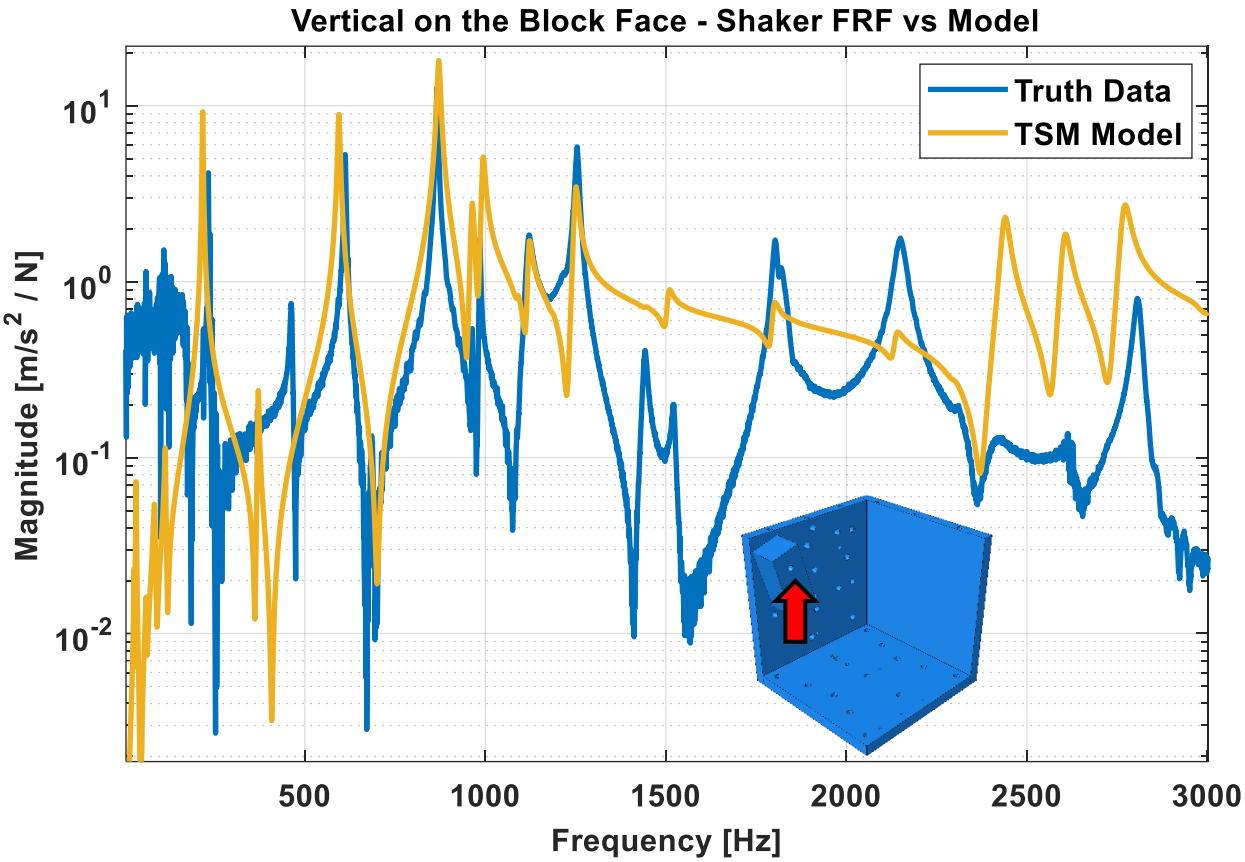

Figure 36: Vertical response on the block face - Shaker excitation FRF vs. model

5.5. Discussion

The final test case demonstrated the effectiveness of the TSM for accounting for significant alterations to the TS dynamics. This was done by combining the half cube TS from test case 2 with the steel block test article from test case 1. As the block does not display any dynamic response in the frequency range utilized, it is effectively a rigid, lumped mass that increases the inertia of the side of the half cube it is attached to, warping the frequencies and modeshapes of the assembly. It was found that, far from the block, on the opposite side of the half cube, the TSM model

produced accurate results past 3000 Hz, through the usable range of the shaker. However, on the half cube directly above the block, the TSM model was only reasonably accurate through approximately 1500 Hz, less than half the range of the other side. Also, when the response at the surface of the block was compared to experimental data from a sin sweep of the shaker, the model also only displayed reasonable accuracy up to near 1300 Hz.

6. Conclusion

This thesis evaluated the transmission simulator method of modal substructuring for the purpose of generating an experimentally based model of an electrodynamic shaker. By implementing this technique, difficulties inherent in attempting to create a FEM of the entire shaker may be circumvented by capturing the effective modal properties of the shaker experimentally, and then coupling arbitrary FEMs of potential test components to this experimental model. Functionally, this will enable alterations to the dynamic behavior of the shaker to be predicted during the pretest phase so one can avoid over- or under-testing components when mounted to the shaker at various locations on the fixture.

To investigate this method, several test cases with various fixtures and test articles of increasing complexity were investigated. In each case, a roving hammer test was performed on the shaker and fixture assembly, producing FRFs to be curve fit, yielding a modal model of the system. After constructing FEMs of the fixture and the fixture with a test article, the TSM could be implemented to generate a model of the shaker, fixture, and the test article.

The first test case served as a proof of concept, with a simple circular aluminum plate as the fixture/TS and a steel block representing a potential test article. The resultant TSM model showed reasonable agreement to experimental truth data up to approximately 3000 Hz, which is the recommended operable frequency range for the shaker. Past this point, numerous small modes present in

the truth data were not created by the TSM. This is believed to be a result of the additional mass of the block possibly causing nonlinear variations to the internal dynamics of the shaker which manifest as the many weak modes visible in the truth data taken on the top of the shaker. This sort of change is unlikely to be replicated by the TSM, as the method assumes that the underlying experimental system behaves linearly.

In the second test case, a three-sided aluminum half cube was implemented as the fixture with an attached cantilever beam as the test article. This setup sought to determine if the response of the half cube could be preserved through the substructuring process of assembling the beam onto the system. It was found that the TSM model could successfully achieve these goals, as the beam and half cube response agreed well with experimental truth data through 3000 Hz.

The final test case essentially combined the first two, in that the steel block from test case 1 was attached to the half cube from test case 2. This setup was designed to cause a significant change to the half cube dynamics and determine if the TSM could accurately predict such a change. It was found that the TSM was able to reproduce the half cube response quite well through 3000 Hz, but only far from the block. Near the steel block, the model yielded inaccurate results past approximately 1500 Hz. This could be a result of the same effects observed in test case 1, in that the addition of the block possibly caused a nonlinear change to the internal shaker dynamics. In this case, it may be a result of the unbalanced mass distribution on the shaker. The center-of-mass of the half cube is biased toward the

vertical sides, even more so toward the block when it is attached. When these are attached to the shaker, the offset mass may induce off axis motion in the shaker, resulting in a response that the TSM likely cannot clearly predict.

As demonstrated in the results for each test case, the TSM is a viable method for modeling an electrodynamic shaker. In order to produce an accurate model, several steps must be completed. Care must be taken in selecting a suitable array of test locations that allow an adequate number of independent modes to be included in the modal basis for each subsystem. Also, to ensure that accurate finite element models are produced, model updating procedures must be done with respect to an experimental model of the physical fixture.

Though promising, the research presented in this thesis offers many avenues for improvements to be explored in future work. To further evaluate the robustness of the TSM for modeling shakers, more elaborate configurations of fixtures and test articles should be tested. This would also allow for further investigation into the effects of fixture and test article distribution on the internal shaker dynamics, and if the TSM is able to predict such changes. Also, there is much work to be done in researching how best to account for damping in this type of substructuring model. This issue was largely ignored in the current work but will be crucial to producing usable models in a nonacademic setting. Also to that end, general metrics to evaluate the generated model are needed to determine the validity of a model when truth data is not known a priori.

References

[1] W. J. DeLima, R. Jones, E. Dodgen and M. Ambrose, "A Numerical Approach to System Model Identification of Random Vibration Test," in *Proceeding of 35th IMAC*, Garden Grove, California, 2017.

[2] W. J. DeLima and M. Ambrose, "Experimental Characterization and Simulation of Vibration Environmental Test," in *Proceedings of the 33rd IMAC*, Orlando, Florida, 2015.

[3] S. Ricci, B. Peeters, R. Fetter, D. Boland and J. Debille, "Virtual shaker testing for predicting and improving," in *Proceedings of the 27th IMAC*, Orlando, Florida, 2009.

[4] M. S. Allen, R. L. Mayes and E. J. Bergman, "Experimental Modal Substructuring to Couple and Uncouple Substructures with Flexible Fixtures and Multi-point Connections," *Journal of Sound and Vibration,* vol. 329, p. 4891–4906, 2010.

[5] R. L. Mayes and M. Arviso, "Design Studies for the Transmission Simulator Method of Experimental Dynamic Substructuring," in *International Seminar on Modal Analysis*, Lueven, Belgium, 2010.

[6] B. Moldenhauer, M. S. Allen, W. J. DeLima and E. Dodgen, "Modeling an Electrodynamic Shaker using Experimental Substructuring," in *Proceedings of the 36th IMAC*, Orlando, Florida, 2018.

[7] B. Moldenhauer, M. S. Allen, W. J. DeLima and E. Dodgen, "Using Hybrid Modal Substructuring with a Complex Transmission Simulator to Model an Electrodynamic Shaker," in *Proceedings of the 37th IMAC*, Orlando, Florida, 2019.

[8] "Dynamic Substructuring Wiki," [Online]. Available: http://substructure.engr.wisc.edu.

[9] D. de Klerk and e. al., "General framework for dynamic substructuring: History, review, and classification of techniques," *AIAA Journal,* vol. 46, pp. 1169-1181, 2008.

[10] M. S. Allen and R. L. Mayes, "Comparison of FRF and Modal Methods for Combining Experimental and Analytical Substructures," in *Proceedings of the 25th IMAC*, Orlando, Florida, 2007.

[11] D. R. Roettgen, M. S. Allen and R. L. Mayes, "Wind Turbine Substructuring using the Transmission Simulator Method," *Sound and Vibration,* November 2016.

[12] M. S. Allen and J. H. Ginsberg, "A Global, Single-Input-Multi-Output (SIMO) Implementation of The Algorithm of Mode Isolation and Applications to

Analytical and Experimental Data," *Mechanical Systems and Signal Processing,* vol. 20, p. 1090–1111, 2006.

[13] M. S. Allen and J. H. Ginsberg, "Global, hybrid, MIMO implementation of the algorithm of mode isolation," in *Proceedings of the 23rd IMAC*, Orlando, Florida, 2005.

[14] M. S. Allen, D. C. Kammer and R. L. Mayes, "Metrics for diagnosing negative mass and stiffness when uncoupling experimental and analytical substructures," *Journal of Sound and Vibration,* vol. 331, p. 5435–5448, 2012.

[15] R. L. Mayes, M. S. Allen and D. C. Kammer, "Correcting Indefinite Mass Matrices Due to Substructure," *Journal of Sound and Vibration,* vol. 332, pp. 5856-5866, 2013.

[16] D. C. Kammer, "Sensor placement for on-orbit modal identification and correlation of large space structures," *Journal of Guidance, Control, and Dynamics,* vol. 14, no. 2, pp. 251-259, 1991.